GEOVision
geophysical services

REPORT
SEISMIC REFRACTION SURVEY

Reds Meadow Road Improvements
Madera County, California

GEO*Vision* Project No. 18419

Prepared for

Shannon & Wilson, Inc.
664 W. Broadway
Glendale, CA 91204
818-539-8408

Prepared by

GEO*Vision* Geophysical Services, Inc.
1124 Olympic Drive
Corona, CA 92881
951-549-1234

November 16, 2018

Report 18419-01

TABLE OF CONTENTS

1 INTRODUCTION 3

2 EQUIPMENT AND FIELD PROCEDURES 4

3 METHODOLOGY 5

4 DATA REDUCTION AND MODELING 7

5 RESULTS 8

5.1 P-WAVE SEISMIC REFRACTION LINE S-1 8
5.2 P-WAVE SEISMIC REFRACTION LINE S-2 9
5.3 P-WAVE SEISMIC REFRACTION LINE S-3 9
5.4 P-WAVE SEISMIC REFRACTION LINE S-4 9
5.5 P-WAVE SEISMIC REFRACTION LINE S-5 10
5.6 P-WAVE SEISMIC REFRACTION LINE S-6 10
5.7 P-WAVE SEISMIC REFRACTION LINE S-7 10
5.8 P-WAVE SEISMIC REFRACTION LINE S-8 10
5.9 P-WAVE SEISMIC REFRACTION LINE S-9 11
5.10 P-WAVE SEISMIC REFRACTION LINE S-10 11
5.11 P-WAVE SEISMIC REFRACTION LINE S-11 11
5.12 P-WAVE SEISMIC REFRACTION LINE S-12 11
5.13 P-WAVE SEISMIC REFRACTION LINE S-13 12
5.14 P-WAVE SEISMIC REFRACTION LINE S-14 12
5.15 P-WAVE SEISMIC REFRACTION LINE S-15 13

6 REFERENCES 14

7 CERTIFICATION 15

LIST OF TABLES

Table 1 Seismic Line Geometry

LIST OF FIGURES

Figure 1-1 Site Map: S-1, S-2, S-3, S-4, S-13
Figure 1-2 Site Map: S-5, S-6, S-7, S-15
Figure 1-3 Site Map: S-8, S-9, S-14
Figure 1-4 Site Map: S-10, S-11, S-12
Figure 2 S-1: P-wave Time-Term Tomography Model
Figure 3 S-2: P-wave Time-Term Tomography Model
Figure 4 S-3: P-wave Time-Term Tomography Model
Figure 5 S-4: P-wave Time-Term Tomography Model
Figure 6 S-5: P-wave Time-Term Tomography Model
Figure 7 S-6: P-wave Time-Term Tomography Model
Figure 8 S-7: P-wave Time-Term Tomography Model
Figure 9 S-8: P-wave Time-Term Tomography Model
Figure 10 S-9: P-wave Time-Term Tomography Model
Figure 11 S-10: P-wave Time-Term Tomography Model
Figure 12 S-11: P-wave Time-Term Tomography Model
Figure 13 S-12: P-wave Time-Term Tomography Model
Figure 14 S-13: P-wave Time-Term Tomography Model
Figure 16 S-14: P-wave Time-Term Tomography Model
Figure 17 S-15: P-wave Time-Term Tomography Model

APPENDICES

Appendix A Technical Note - Seismic Refraction Method

1 INTRODUCTION

A P-wave seismic refraction survey was conducted along Reds Meadow Road near Reds Meadow in Madera County, California on October 15th through the 20th, 2018. The survey was conducted along fifteen (15) P-wave seismic refraction lines, designated as S-1 through S-15 (Figures 1-1, 1-2, 1-3, and 1-4). The purpose of this investigation was to determine the depth and rippability of rock.

The locations of the lines were generally placed by Shannon & Wilson and modified by **GEO***Vision* to maximize the space available and account for terrain and vegetation. The endpoints of each refraction line were surveyed by **GEO***Vision* personnel using a Spectra Precision SP60 with CenterPoint RTX submeter corrections (Table 1) and plotted on the site maps (Figures 1-1, 1-2, 1-3, and 1-4).

The geology in the vicinity of the seismic refraction lines was expected to consist of fill and colluvium overlying undifferentiated metasedimentary and metavolcanic bedrock. The physical characteristics of the metasedimentary and metavolcanic bedrock, such as fracture spacing, porosity, or density, were unknown.

Ripping characteristics for metasedimentary and metavolcanic rocks are not published and, therefore, ripping characteristics of schist is used for site characteristics. Schist is considered rippable by a Caterpillar D8R Ripper to a P-wave velocity of 6,250 ft/s and marginally rippable to a velocity of 8,250 ft/s providing the rock is sufficiently jointed and fractured. Schist is considered rippable by a Caterpillar D10R Ripper to a velocity of 7,750 ft/s and marginally rippable to a velocity of 9,500 ft/s providing the rock is sufficiently jointed and fractured. It should be noted that blasting may be more cost-effective in marginally rippable rock due to time and equipment wear considerations. Published data are not available for the ripping characteristics of excavators, but we typically assume that excavators have about half the ripping ability of a D8R.

The following sections include a discussion of equipment and field procedures, methodology, data processing, and results of the geophysical survey.

2 EQUIPMENT AND FIELD PROCEDURES

Seismic refraction equipment used during this investigation consisted of two Geometrics Geode 24-channel signal enhancement seismographs, 10 Hz vertical geophones, seismic cables with 10-foot takeouts, a 20-lb and 10-lb sledgehammer, and an aluminum plate.

Each line consisted of a one spread of 24 to 48 geophones aligned in a linear array. The geophone spacing, number of geophones, and total lengths per line are outlined in Table 1. Elevations along the P-wave refraction lines were collected using a Sokkia C300 automatic level and were surveyed using a Spectra Precision SP60 GPS system with CenterPoint RTX submeter, real-time corrections. All geophone locations were measured using a 300 foot tape measure.

A typical seismic refraction survey field layout is shown in Appendix A. Up to fifteen (15) shot point locations were occupied on each P-wave spread: off-end shots (where possible), end shots, and multiple interior shot points located between every third or fourth geophone. Site conditions such as topography and vegetation limited or prohibited the placement of off-end shots. A 10-lb or 20-lb sledgehammer was used as the energy source at each shot point.

A 3D Geophysics hammer switch attached to the sledgehammer and coupled to the Geode via a trigger extension was used to trigger the seismograph upon impact. The final seismic record at each shot point was the result of stacking 4 to 10 shots to increase the signal to noise ratio. All seismic records were stored on a laptop computer. Data files were named with the sequential line, spread, and shot number and a ".dat" extension (e.g. data file 1105.dat is the seismic record from line 1, spread 1, shot 5). Data acquisition parameters, file names, and leveling data were recorded on a field form, which is retained in the project files.

3 METHODOLOGY

Detailed discussions of the seismic refraction method can be found in Telford et al. (1990), Dobrin and Savit (1988), and Redpath (1973).

When conducting a seismic survey, acoustic energy is input to the subsurface by an energy source such as a sledgehammer impacting a metallic plate, weight drop, vibratory source, or explosive charge. The acoustic waves propagate into the subsurface at a velocity dependent upon the elastic properties of the material through which they travel. When the waves reach an interface where the density or velocity changes significantly, a portion of the energy is reflected back to the surface and the remainder is transmitted into the lower layer. Where the velocity of the lower layer is higher than that of the upper layer, a portion of the energy is also critically refracted along the interface. Critically refracted waves travel along the interface at the velocity of the lower layer and continually refract energy back to the surface. Receivers (geophones) laid out in linear array on the surface, record the incoming refracted and reflected waves. The seismic refraction method involves analysis of the travel times of the first energy to arrive at the geophones. These first-arrivals are from either the direct wave (at geophones close to the source) or critically refracted waves (at geophones further from the source).

Analysis of seismic refraction data depends upon the complexity of the subsurface velocity structure. If the subsurface target is planar in nature, then the slope intercept method (Telford et al. [1990]) can be used to model multiple horizontal or dipping planar layers. A minimum of one end shot is required to model horizontal layers and reverse end shots are required to model dipping planar layers. If the subsurface target is undulating (i.e. bedrock valley) then layer-based analysis routines such as the generalized reciprocal method (Palmer [1980 and 1981], Lankston and Lankston [1986], and Lankston [1990]), reciprocal method (Hawkins, 1961) also referred to as the ABC method, Hales' method (Hales, 1958), delay time method (Wyrobek [1956] and Gardner [1967]), time-term inversion (Scheidegger and Willmore, 1957), plus-minus method (Hagedoorn, 1959), and wavefront method (Rockwell, 1967) are required to model subsurface velocity structure. These methods generally require a minimum of 5 shot points per spread (end shots, off-end shots, and a center shot). If subsurface velocity structure is complex and cannot be adequately modeled using layer-based modeling techniques (i.e., complex weathering profile in bedrock, numerous lateral velocity variations), then Monte Carlo or tomographic inversion techniques (Zhang and Toksoz [1998], Schuster and Quintus-Bosz [1993]) are required to model the seismic refraction data. These techniques require a high shot density; typically every 2 to 6 stations/geophones. Generally, these techniques cannot effectively take advantage of off-end shots to extend depth of investigation, so longer profiles are required.

Errors in seismic refraction models can be caused by velocity inversions, hidden layers, or lateral velocity variations. At sites with steeply dipping or highly irregular bedrock surfaces, out of plane refractions (refractions from structures to the side of the line rather than from beneath the line) may severely complicate modeling. A velocity inversion is a geologic layer with a lower seismic velocity than an overlying layer. Critical refraction does not occur along such a layer because velocity has to increase with depth for critical refraction to occur. This type of layer, therefore, cannot be recognized or modeled and depths to underlying layers would be overestimated. A hidden layer is a layer with a velocity increase, but of sufficiently small thickness relative to the velocities of overlying and underlying layers, that refracted arrivals do

not arrive at the geophones before those from the deeper, higher velocity layer. Because the seismic refraction method generally only involves the interpretation of first arrivals, a hidden layer cannot be recognized or modeled and depths to underlying layers would be underestimated. Saturated sediments, overlying high velocity bedrock can be a hidden layer under many field conditions. However, saturated sediments generally have a much higher velocity than unsaturated sediments, typically in the 5,000 to 7,000 ft/s range, and can occasionally be interpreted as a second arrival when the layer does not give rise to a first arrival. A subsurface velocity structure that increases as a function of depth rather than as discrete layers will also cause depths to subsurface refractors to be underestimated, in a manner very similar to that of the hidden layer problem. Lateral velocity variations that are not adequately addressed in the seismic models will also lead to depth errors. Tomographic imaging techniques can often resolve the complex velocity structures associated with hidden layers, velocity gradients, and lateral velocity variations. However, in the event of an abrupt increase in velocity at a geologic horizon, the velocity model generated using tomographic inversion routines will smooth the horizon with velocity being underestimated at the interface and possibly overestimated at depth.

4 DATA REDUCTION AND MODELING

The first step in data processing consisted of picking the arrival time of the first energy received at each geophone (first-arrival) for each shot point. The first-arrivals on each seismic record are either a direct arrival from a compressional (P) wave traveling in the uppermost layer or a refracted arrival from a subsurface interface where there is a velocity increase. First-arrival times were selected using the automatic and manual picking routines in the software package SeisImager™ (Oyo Corporation). These first-arrival times were saved in an ASCII file containing shot location, geophone locations, and associated first-arrival time.

Relative elevations for each geophone location were calculated from the leveling data using a spreadsheet and converted to approximate elevations using the elevation recorded from the GPS at the ends of each line.

Data quality was affected by factors such as: topography, geologic conditions, wind, and nearby noise (e.g. fire helicopters). Errors in the first arrival times were variable with error generally increasing with distance from the shot point.

Seismic refraction data were then modeled using the tomographic analysis technique available in the SeisImager™ Plotrefa software package, developed by Oyo Corporation. Refraction tomography techniques are often able to resolve complex velocity structure (e.g. velocity gradients) that can be observed in bedrock weathering profiles. Layer-based modeling techniques such as GRM are not able to accurately model the velocity gradients that can be observed in weathered or transitional zones.

Tomographic analysis was conducted in several steps. First, an initial model was generated using a smooth or layer-based (i.e. time-term) starting model. The initial model was then converted to 20 layers with the top of the bottom layer at a depth related to the imaged depth of the model. Velocity ranges were also set to values outside of the starting model minimum and maximum. A minimum of 50 iterations of non-linear raypath inversion were then implemented to improve the fits of the travel time curves to near-surface sediments/rock. After each set of inversions were completed, the initial parameters were adjusted and the model run again in an iterative process. These steps were repeated until acceptable fits and RMS error were achieved. The final tomographic velocity models for the seismic line were exported as ASCII files and imported into the Geosoft Oasis montaj® v9 mapping system where the velocity model was gridded, contoured, and annotated for presentation.

5 RESULTS

The layer-based, time-term starting, P-wave seismic tomography models for S-1 through S-15 are presented as Figures 2 through 16, respectively. The color scheme used on the tomography images consists of blue-green, yellow-orange, and red-pink representing low, intermediate, and high velocities, respectively. The transition from blue to cyan occurs at a P-wave seismic velocity of 1,000 ft/s and the transition from green to yellow occurs at a velocity of 4,500 ft/s. The transition from orange to red occurs at 7,000 ft/s. It is expected that either the rock is very close to the surface or very soft fill and colluvium overlie a hard rock interface which is more suitable for layer-based modeling techniques. For the seismic refraction lines, time-term based starting models were used to retain the observed layered structure while still showing velocity gradients, which may indicate variable zones of weathering.

Tomographic inversion techniques will typically model a gradual increase in velocity with depth even if an abrupt velocity contact is present. Therefore, if velocity gradients are not present, tomographic inversion routines will overestimate and underestimate velocity above and below a layer contact, respectively. In these cases layer-based techniques, such as time-term, may be better suited estimating rock velocity to determine rippability characteristics. Velocity gradients can, however, be very common in geologic environments with fractured or weathered rock, such as the project site. In tomographic images, layer contacts are not clearly defined and thus, ranges of velocities are used to interpret possible rock conditions and competency.

For this survey, the top of bedrock is generally interpreted at the 4,000 to 5,000 ft/s contours for Lines S-4 through S-15. For lines S-1, S-2, and S-3 top of bedrock is interpreted at the 2,000 to 3000 ft/s contours which indicates that rock is likely more weathered or fractured in this portion of the site. These contours were selected to approximately match the depths of rock interpreted in the geologic borehole data in the vicinity of the lines. Groundwater was not expected to be encountered on any of the seismic lines. A black dashed line is shown on the seismic tomography models indicating the interpreted interface between the fill/colluvium and bedrock. For the purpose of discussion, velocities of 6,000 ft/s or less are considered rippable, velocities of 6,000 to 8,000 ft/s are considered marginally rippable, and velocities greater than 8,000 ft/s are considered non-rippable using a Caterpillar D8R Ripper.

5.1 P-Wave Seismic Refraction Line S-1

The time-term tomography model for S-1 is presented as Figure 2. S-1 was located in the southern portion of the site and aligned roughly west to east on the northern side of Reds Meadow Road (Figure 1-1). The primary purpose of the S-1 was to determine bedrock rippability characteristics. Overall, this line is imaged with a thick and uneven weathering profile. The weathered rock is imaged very near the surface along the western and central portions of the line, and 7 to 10 ft below the surface beneath the eastern portion of the line. Shallow, harder rock is imaged between 60 and 125 ft along the line and may be related to less weathering of the outcrop in the area. Competent rock (velocities above 8,000 ft/s) was not imaged within the depth of investigation, about 50 ft, in the model for S-1. Marginally rippable bedrock, with velocities greater than 6,000 ft/s was imaged approximately 23 to 35 ft beneath the western and central portions of the line. However, velocities are expected to increase with depth and may exceed 6,000 ft/s shortly below a depth of 50 ft beneath the eastern portion of the line.

Velocities do not appear to exceed 8,000 ft/s, and therefore the modeled data is considered rippable to marginally rippable by a D8R Ripper.

5.2 P-Wave Seismic Refraction Line S-2

The time-term tomography model for S-2 is presented as Figure 3. S-2 was located in the southern portion of the site and aligned roughly south to north on the western side of Reds Meadow Road (Figure 1-1). Also, S-2 is roughly parallel to S-3, which is located on the eastern side of Reds Meadow Road. The model for S-2 had the highest error of all lines modeled. This may be due to out-of-plane refractors or asphalt arrivals that could not be separated from geologic arrivals. The primary purpose of S-2 was to determine depth to bedrock. The interpreted top of weathered rock is imaged at a depth of about 14 to 17 ft beneath the southern portion, 12 ft beneath the central portion, and 10 ft beneath the northern portion of the seismic line. Borehole S-W-B6 was drilled along the southern portion of S-2 and encountered rock at a depth of 14 ft which agrees well with the interpreted top of bedrock.

The northern portion of the line displays higher velocity material which may indicate less weathering of rock. It is possible that asphalt arrival contamination of the northern portion of the line may contribute to higher velocities. Line S-3, which runs parallel and east of S-2, also shows higher velocities in the northern portion of the model but does not have the same depth imaged in that area. If not affected by asphalt contamination, the material is considered marginally rippable where the velocities reach 6,000 ft/s at a depth of about 35 ft for the northern portion of the line. At a depth of about 38 ft, where the material reaches a velocity of greater than 8,000 ft/s, the rock is considered non-rippable by a D8R Ripper. It should also be noted that, higher velocities are imaged at the edge of the model and may also be influenced by modeling edge effects.

5.3 P-Wave Seismic Refraction Line S-3

The time-term tomography model for S-3 is presented as Figure 4. S-3 was located in the southern portion of the site and aligned roughly south to north on the eastern side of Reds Meadow Road (Figure 1-1). Also, S-3 is roughly parallel to S-2, which is located on the western side of Reds Meadow Road. The primary purpose of the S-3 was to determine depth to bedrock. The interpreted top of the weathered rock is imaged at a depth of about 7 to 9 ft beneath the southern portion, 3 to 6 ft beneath the central portion, and 1 to 2 ft beneath the northern portion of the seismic line. The velocities in the model do not exceed 5,200 ft/s and therefore, all the material imaged in the modeled data is considered rippable by a D8R Ripper.

5.4 P-Wave Seismic Refraction Line S-4

The time-term tomography model for S-4 is presented as Figure 5. S-4 was located in the southern portion of the site and aligned roughly south to north, above the eastern side of Reds Meadow Road on an outcrop (Figure 1-1). The primary purpose of the S-4 was to determine bedrock rippability characteristics. Overall, this line is imaged with soil and colluvium overlying fairly shallow bedrock. The interpreted bedrock is imaged 5 to 12 ft beneath the southern portion and 8 to 10 ft beneath the central and northern portions of the line. A zone of harder rock is imaged between 40 and 80 ft along the line and may be related to less weathering beneath this portion of the line. Based on field observations, rock was at the surface or very near surface along the southern portion of the line, which is not shown on the seismic tomography model.

This may be related to rock occurring near the edge of the model and consequently poorly constrained.

Seismic velocities do not appear to exceed 6,000 ft/s (rippable material) until a depth of about 8 to 16 ft beneath the southern portion, 10 to 12 ft beneath the central portion, and 10 to 17 ft beneath the northern portion of the line. However, the time-term seismic model images bedrock with a velocity of about 7,500 ft/s which is considered marginally rippable providing the rock is sufficiently jointed and fractured. This is likely related to velocity smoothing inherent in tomographic velocity models. For planning purposes, bedrock beneath this line should be considered marginally rippable to non-rippable by a D8R Ripper.

5.5 P-Wave Seismic Refraction Line S-5

The time-term tomography model for S-5 is presented as Figure 6. S-5 was located in the southern portion of the site and aligned roughly southwest to northeast on the western side of Reds Meadow Road (Figure 1-2). The primary purpose of S-5 was to determine depth to bedrock. The interpreted top of the bedrock is imaged at a depth of about 9 to 15 ft beneath the southwestern portion and about 15 ft beneath the central and northeastern portions of the seismic line. Overall, this line is imaged with bedrock becoming shallower to the southwest. Borehole S-W-B7 was located south of seismic line and encountered rock at a depth of 6.5 ft which suggests that bedrock is indeed becoming shallower to the south, outside the range of the line.

5.6 P-Wave Seismic Refraction Line S-6

The time-term tomography model for S-6 is presented as Figure 7. S-6 was located in the southern central portion of the site and aligned roughly west to east. The eastern end of S-6 is located on the western edge of Reds Meadow Road (Figure 1-2) and the line runs downhill to the west. The primary purpose of S-6 was to determine depth to bedrock. The interpreted top of the bedrock is imaged at a depth of about 16 to 18 ft beneath the western portion and 12 to 14 ft beneath the central and eastern portions of the seismic line. Borehole S-W-B10 was located on Reds Meadow Road near the eastern end of S-6. S-W-B10 encountered rock at a depth of 14 ft which agrees with the interpreted top of bedrock.

5.7 P-Wave Seismic Refraction Line S-7

The time-term tomography model for S-7 is presented as Figure 8. S-7 was located in the central portion of the site and aligned roughly southwest to northeast. The northeastern end of S-7 is located on the western edge of Reds Meadow Road (Figure 1-2) and the line runs downhill to the southwest. The primary purpose of S-7 was to determine depth to bedrock. The interpreted top of the bedrock is imaged at a depth of about 8 to 10 ft beneath the southwestern and central portions and, 10 to 13 ft beneath the northeastern portions of the seismic line. Borehole S-W-B12 was located on Reds Meadow Road around the eastern end of S-7. S-W-B12 encountered rock at a depth of 13 ft which agrees with the interpreted top of bedrock.

5.8 P-Wave Seismic Refraction Line S-8

The time-term tomography model for S-8 is presented as Figure 9. S-8 was located in the central portion of the site and aligned roughly south to north, above the eastern side of Reds Meadow Road on an outcrop (Figure 1-3). The primary purpose of the S-8 was to determine bedrock

rippability characteristics. Overall, this line is imaged with undulating shallow bedrock. The interpreted bedrock is imaged 1 to 5 ft beneath the southern portion and 6 to 10 ft beneath the central and northern portions of the line. A zone of harder rock is imaged with velocities exceeding 10,000 ft/s at a depth of about 20 ft along northern portion of the line and may be related to less weathering in the area.

Seismic velocities do not appear to exceed 8,000 ft/s (non-rippable material) until depths on the order of 15 to 30 ft shown on the tomography model. However, the time-term seismic model images bedrock with a velocity of about 9,200 ft/s at depths corresponding to the interpreted top of bedrock which is considered non-rippable. This is likely related to velocity smoothing inherent in tomographic velocity models. For planning purposes, bedrock beneath this line should be considered non-rippable by a D8R Ripper.

5.9 P-Wave Seismic Refraction Line S-9

The time-term tomography model for S-9 is presented as Figure 10. S-9 was located in the central northern portion of the site and aligned roughly west to east. The eastern end of S-9 is located on the western side of Reds Meadow Road (Figure 1-3) and the line runs downhill to the west. The primary purpose of S-9 was to determine depth to bedrock. The interpreted top of the bedrock is imaged at a depth of about 7 to 17 ft beneath the western portion, 20 to 25 ft beneath the central portion, and 15 to 20 ft beneath the eastern portion of the seismic line. Borehole S-W-B16 was located on Reds Meadow Road off the eastern end of S-9. S-W-B16 encountered rock at a depth of 14 ft which agrees with the interpreted top of bedrock. It should also be noted, that the interpreted top of bedrock is imaged near the depth of investigation, about 25 to 30 ft, and may not be well constrained by the seismic tomography model.

5.10 P-Wave Seismic Refraction Line S-10

The time-term tomography model for S-10 is presented as Figure 11. S-10 was located in the northern portion of the site and aligned roughly northwest to southeast. S-10 was conducted at the approximate toe of fill material, below the western side of Reds Meadow Road (Figure 1-4). The primary purpose of S-10 was to determine depth to bedrock. The interpreted top of the bedrock is imaged at a depth of about 19 to 21 ft beneath the northwestern portion, 20 to 22 ft beneath the central portion, and 13 to 18 ft beneath the eastern portion of the seismic line.

5.11 P-Wave Seismic Refraction Line S-11

The time-term tomography model for S-11 is presented as Figure 12. S-11 was located in the northern portion of the site and aligned roughly southwest to northeast. The northeastern end of S-11 is located on the western side of Reds Meadow Road (Figure 1-4) and the line runs downhill to the southwest. The primary purpose of S-11 was to determine depth to bedrock. The interpreted top of the bedrock is imaged at a depth of about 8 to 10 ft beneath the seismic line. Borehole S-W-B20 was located on Reds Meadow Road off the eastern end of S-11. S-W-B20 encountered rock at a depth of 7.5 ft which agrees with the interpreted top of bedrock.

5.12 P-Wave Seismic Refraction Line S-12

The time-term tomography model for S-12 is presented as Figure 13. S-12 was located in the northern portion of the site and aligned roughly northwest to southeast, above the eastern side of

Reds Meadow Road on an outcrop (Figure 1-3). The primary purpose of the S-12 was to determine bedrock rippability characteristics. Overall, this line is imaged with undulating shallow bedrock. The interpreted bedrock is imaged 3 to 6 ft beneath the northwest portion, at the surface to 3 ft beneath the central portion, and 3 to 8 ft beneath the southeastern portions of the line.

Seismic velocities do not appear to exceed 8,000 ft/s (non-rippable material) till depths on the order of 5 to 12 ft shown on the tomography model. At the interpreted top of bedrock the velocities may reach 10,700 ft/s based on the time-term modeled velocities. The variation in bedrock velocities may be due to velocity smoothing inherent in tomographic velocity models. For planning purposes, bedrock beneath this line should be considered non-rippable by a D8R Ripper.

5.13 P-Wave Seismic Refraction Line S-13

The time-term tomography model for S-13 is presented as Figure 14. S-13 was located in the southern portion of the site and aligned roughly southeast to northwest, above the eastern side of Reds Meadow Road on an outcrop (Figure 1-1). The primary purpose of the S-13 was to determine bedrock rippability characteristics. Overall, this line is imaged with soil and colluvium overlying fairly shallow bedrock. The interpreted bedrock is imaged 7 to 10 ft beneath the southeastern portion, 3 to 6 ft beneath the central portion, and 7 to 9 ft beneath the northwestern portions of the line. Based on field observations, rock was at the surface or very near surface at the northwestern end of the line, which is not shown on the seismic tomography model. This may be related to rock occurring near the edge of the model and consequently poorly constrained.

Seismic velocities do not appear to exceed 8,000 ft/s (non-rippable material) until a depth of about 13 to 23 ft beneath the southeastern portion, 10 to 28 ft beneath the central portion, and about 10 ft beneath the northwestern portion of the line. However, the time-term seismic model images bedrock with a velocity of about 8,700 ft/s which is considered non-rippable. This is likely related to velocity smoothing inherent in tomographic velocity models. For planning purposes, bedrock beneath this line should be considered non-rippable by a D8R Ripper.

5.14 P-Wave Seismic Refraction Line S-14

The time-term tomography model for S-14 is presented as Figure 15. S-14 was located in the central northern portion of the site and aligned roughly west to east. The eastern end of S-14 is located on the western edge of Reds Meadow Road (Figure 1-3) and the line runs downhill to the west. The primary purpose of S-14 was to determine depth to bedrock. The interpreted top of the bedrock is imaged at a depth of about 28 ft beneath the western portion, 22 to 25 ft beneath the central portion, and 12 to 15 ft beneath the eastern portion of the seismic line. Borehole S-W-B49 was located on Reds Meadow Road in the vicinity of the eastern end of S-14. S-W-B49 encountered rock at a depth of 18.5 ft which does not agree well with the interpreted top of bedrock. However, the seismic line was located on a ridge and the borehole was located near a drainage. These structurally divergent areas are expected to have different depths of bedrock, where bedrock would likely be deeper near the drainage.

5.15 P-Wave Seismic Refraction Line S-15

The time-term tomography model for S-15 is presented as Figure 16. S-15 was located in the central portion of the site and aligned roughly south to north. S-15 was conducted at the approximate toe of fill material, below the western side of Reds Meadow Road (Figure 1-2). The primary purpose of S-15 was to determine depth to bedrock. The interpreted top of the bedrock is imaged at a depth of about 6 to 7 ft beneath the south and central portion, and 5 ft beneath the northern portion of the seismic line. Borehole S-W-B11 was located at a higher elevation on Reds Meadow Road in the vicinity of the seismic line. S-W-B11 did not encountered rock within the upper 13.5 ft; however, the seismic line was conducted at a lower elevation, below the 13.5 ft logged in the borehole.

6 REFERENCES

Dobrin, M.S., and Savit, J., 1988, Introduction to Geophysical Prospecting, McGraw-Hill Co., New York.

Gardner, L.W., 1967, Refraction seismograph profile interpretation, in Musgrave, A.W., ed., Seismic Refraction Prospecting: Society of Exploration Geophysicists, p. 338-347.

Hales, F. W., 1958, An accurate graphical method for interpreting seismic refraction lines: Geophysical Prospecting, v. 6, p 285-294.

Hagedoorn, J.G., 1959, The plus-minus method of interpreting seismic refraction sections, Geophysical Prospecting, v. 7, p 158-182.

Hawkins, L. V., 1961, The reciprocal method of routine shallow seismic refraction investigation: Geophysics, v. 26, p. 806-819.

Lankston, R. W., 1990, High-resolution refraction seismic data acquisition and interpretation, in Ward, S. H., ed., Geotechnical and Environmental Geophysics, Volume I: Review and Tutorial: Society of Exploration Geophysicists, Tulsa, Oklahoma, p. 45-74.

Lankston, R. W., and Lankston, M. M., 1986, Obtaining multilayer reciprocal times through phantoming, Geophysics, v. 51, p. 45-49.

Palmer, D., 1980, The generalized reciprocal method of seismic refraction interpretation: Society of Exploration Geophysics, Tulsa, Oklahoma, 104 p.

Palmer, D., 1981, An introduction to the field of seismic refraction interpretation: Geophysics, v. 46, p. 1508-1518.

Redpath, B. B., 1973, Seismic refraction exploration for engineering site investigations: U. S. Army Engineer Waterway Experiment Station Explosive Excavation Research Laboratory, Livermore, California, Technical Report E-73-4, 51 p.

Rockwell, D.W. 1967. A general wavefront method. In Seismic Refraction Prospecting, A.W. Musgrave, ed., pp 363-415. Tulsa: Society of Exploration Geophysicists.

Scheidegger, A., and Willmore, P.L., 1957, The use of a least square method for the interpretation of data from seismic surveys, Geophysics, v. 22, p. 9-22.

Schuster, G. T. and Quintus-Bosz, A., 1993, Wavepath eikonal traveltime inversion: Theory: Geophysics, v. 58, no. 9, p. 1314-1323.

Telford, W. M., Geldart, L.P., Sheriff, R.E., 1990, Applied Geophysics, Second Edition, Cambridge University Press.

Wyrobek, S.M., 1956, Application of delay and intercept times in the interpretation of multilayer time distance curves, Geophysical Prospecting, v. 4, p 112-130.

Zhang, J. and Toksoz, M. N., 1998, Nonlinear refraction traveltime tomography, Geophysics, V. 63, p. 1726-1737.

7 CERTIFICATION

All geophysical data, analysis, interpretations, conclusions, and recommendations in this document have been prepared under the supervision of and reviewed by a **GEO***Vision* California Professional Geophysicist.

Prepared by

11/16/18

William Dalrymple
California Professional Geophysicist, P.Gp. 1072
GEO*Vision* Geophysical Services

Date

and

11/16/18

David Carpenter
California Professional Geophysicist, P.Gp. 1088
GEO*Vision* Geophysical Services

Date

* This geophysical investigation was conducted under the supervision of a California Professional Geophysicist using industry standard methods and equipment. A high degree of professionalism was maintained during all aspects of the project from the field investigation and data acquisition, through data processing, interpretation, and reporting. All original field data files, field notes, and observations, and other pertinent information are maintained in the project files and are available for the client to review for a period of at least one year.

  A professional geophysicist's certification of interpreted geophysical conditions comprises a declaration of his/her professional judgment. It does not constitute a warranty or guarantee, expressed or implied, nor does it relieve any other party of its responsibility to abide by contract documents, applicable codes, standards, regulations, or ordinances.

TABLES

Table 1 Seismic Line Geometry

Name	Spacing (ft)	Channels	Location (ft)	Northing (US Feet)	Easting (US Feet)	Latitude	Longitude
S-1	5	48	0	2,063,536	6,978,444	37.65326	-119.06027
			235	2,063,627	6,978,656	37.65350	-119.05953
S-2	6	24	0	2,064,769	6,977,318	37.65670	-119.06410
			138	2,064,900	6,977,278	37.65706	-119.06423
S-3	5	24	0	2,064,773	6,977,335	37.65671	-119.06404
			115	2,064,884	6,977,307	37.65701	-119.06413
S-4	5	44	0	2,065,336	6,977,091	37.65826	-119.06485
			215	2,065,546	6,977,125	37.65884	-119.06472
S-5	5	24	0	2,065,788	6,977,072	37.65950	-119.06489
			115	2,065,896	6,977,112	37.65980	-119.06475
S-6	5	24	0	2,066,823	6,977,097	37.66235	-119.06475
			115	2,066,870	6,977,193	37.66247	-119.06442
S-7	5	24	0	2,067,690	6,976,752	37.66474	-119.06590
			115	2,067,765	6,976,825	37.66494	-119.06564
S-8	5	48	0	2,068,711	6,976,033	37.66757	-119.06833
			235	2,068,922	6,975,935	37.66816	-119.06865
S-9	5	24	0	2,069,685	6,975,534	37.67027	-119.07000
			115	2,069,664	6,975,641	37.67021	-119.06963
S-10	5	24	0	2,071,204	6,975,022	37.67446	-119.07169
			115	2,071,134	6,975,085	37.67427	-119.07147
S-11	5	24	0	2,071,550	6,974,403	37.67544	-119.07381
			115	2,071,621	6,974,474	37.67563	-119.07356
S-12	6	24	0	2,072,606	6,973,372	37.67838	-119.07732
			138	2,072,552	6,973,486	37.67823	-119.07692
S-13	5	48	0	2,065,053	6,977,183	37.65748	-119.06455
			235	2,065,258	6,977,081	37.65805	-119.06489
S-14	5	24	0	2,070,107	6,975,579	37.67143	-119.06982
			115	2,070,135	6,975,679	37.67150	-119.06948
S-15	5	24	0	2,067,102	6,977,078	37.66311	-119.06480
			115	2,067,219	6,977,054	37.66343	-119.06488

Notes:

1. Plane coordinates in CA State Plane, Zone III (0403), NAD83 (Conus), US Survey Feet.
2. Geodetic coordinates in WGS84.
3. Coordinates taken with a Spectra Precision SP60 with CenterPoint RTX submeter corrections.

FIGURES

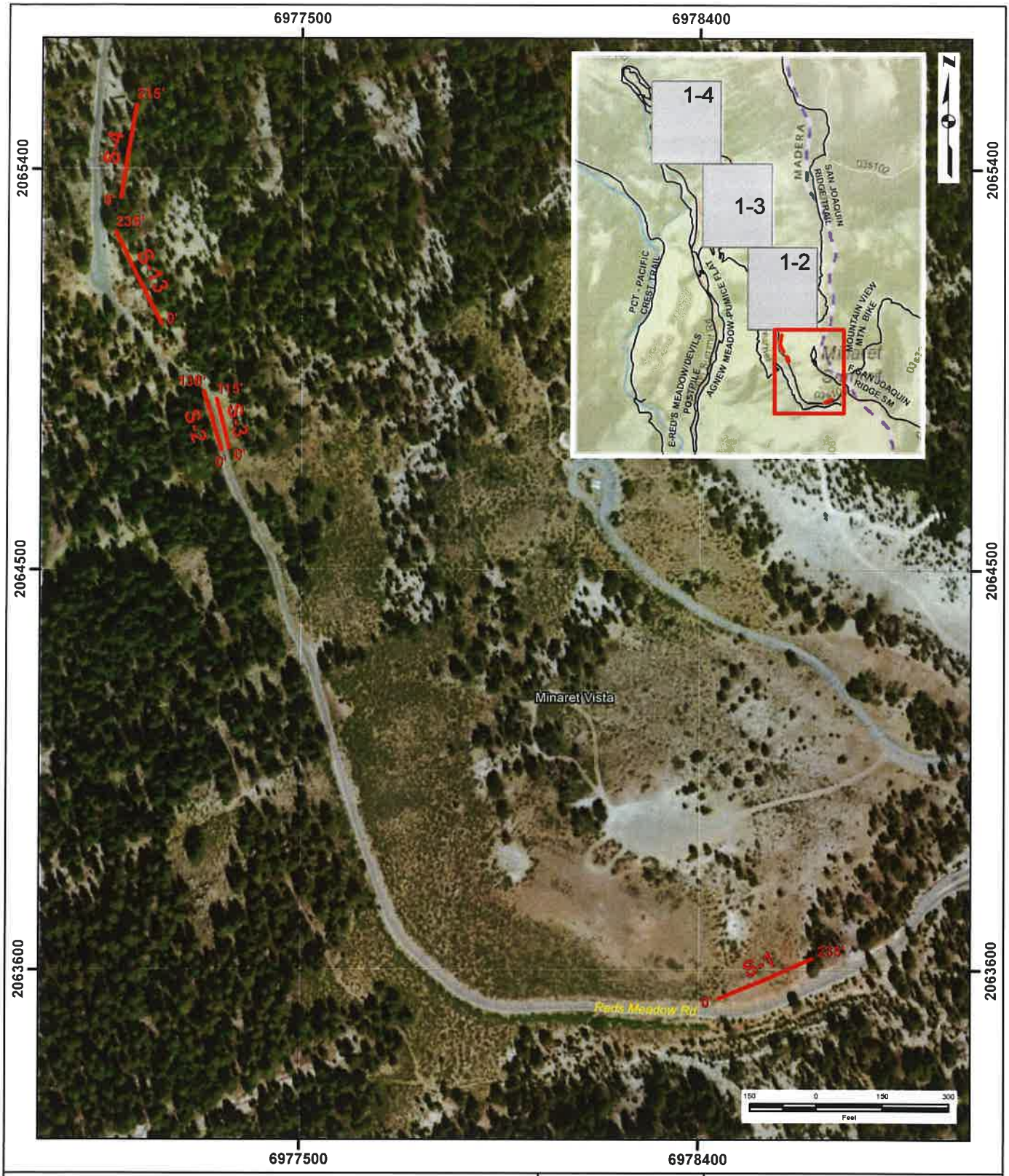

Legend

P-wave Seismic Refraction Line

NOTES:
1. California State Plane Coordinate System, NAD 83, Zone III (0403), US Survey Feet
2. Base map source: Esri, DigitalGlobe, GeoEye, Earthstar Geographics, CNES/Airbus DS, USDA, USGS, AeroGRID, IGN, HERE, Garmin, Intermap, increment P Corp., GEBCO, FAO, NPS, NRCAN, GeoBase,Kadaster NL, Ordnance Survey, Esri Japan, METI, Esri China (Hong Kong), swisstopo, © OpenStreetMap contributors, and the GIS User Community

GEOVision geophysical services

Date:	11/7/2018
GV Project:	18419
Developed by:	D Carpenter
Drawn by:	T Rodriguez
Approved by:	W Dalrymple
File Name:	18419_1.MXD

FIGURE 1-1
S-1, S-2, S-3, S-4, S-13

SITE LOCATED NEAR
REDS MEADOW
MADERA COUNTY, CALIFORNIA

PREPARED FOR
SHANNON & WILSON, INC.

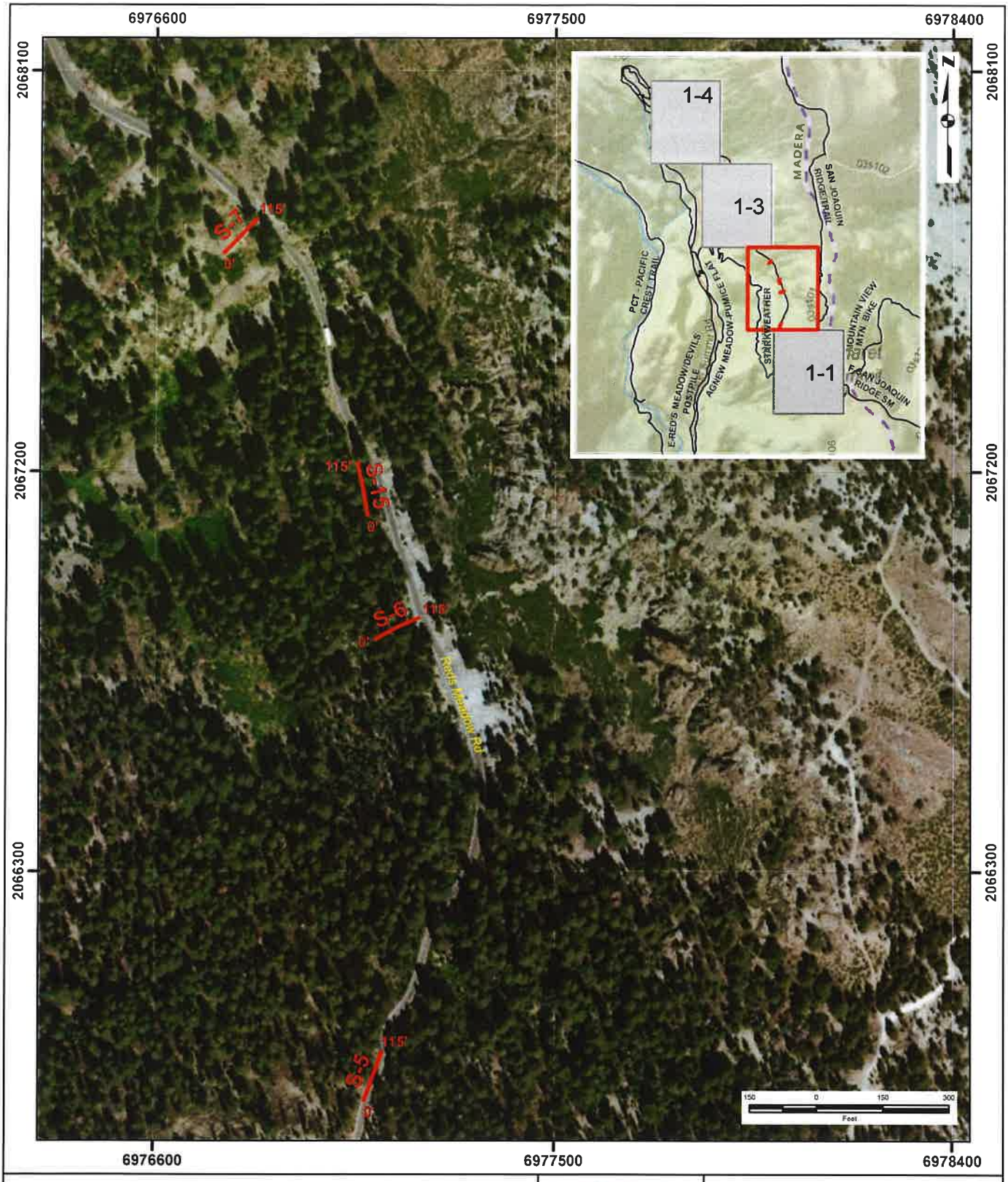

Legend

— P-wave Seismic Refraction Line

NOTES:
1. California State Plane Coordinate System, NAD 83, Zone III (0403), US Survey Feet
2. Base map source: Esri, DigitalGlobe, GeoEye, Earthstar Geographics, CNES/Airbus DS, USDA, USGS, AeroGRID, IGN, HERE, Garmin, Intermap, increment P Corp., GEBCO, FAO, NPS, NRCAN, GeoBase,Kadaster NL, Ordnance Survey, Esri Japan, METI, Esri China (Hong Kong), swisstopo, © OpenStreetMap contributors, and the GIS User Community

GEOVision geophysical services

Date:	11/7/2018
GV Project:	18419
Developed by:	D Carpenter
Drawn by:	T Rodriguez
Approved by:	W Dalrymple
File Name:	18419_1.MXD

FIGURE 1-2
S-5, S-6, S-7, S-15

SITE LOCATED NEAR
REDS MEADOW
MADERA COUNTY, CALIFORNIA

PREPARED FOR
SHANNON & WILSON, INC.

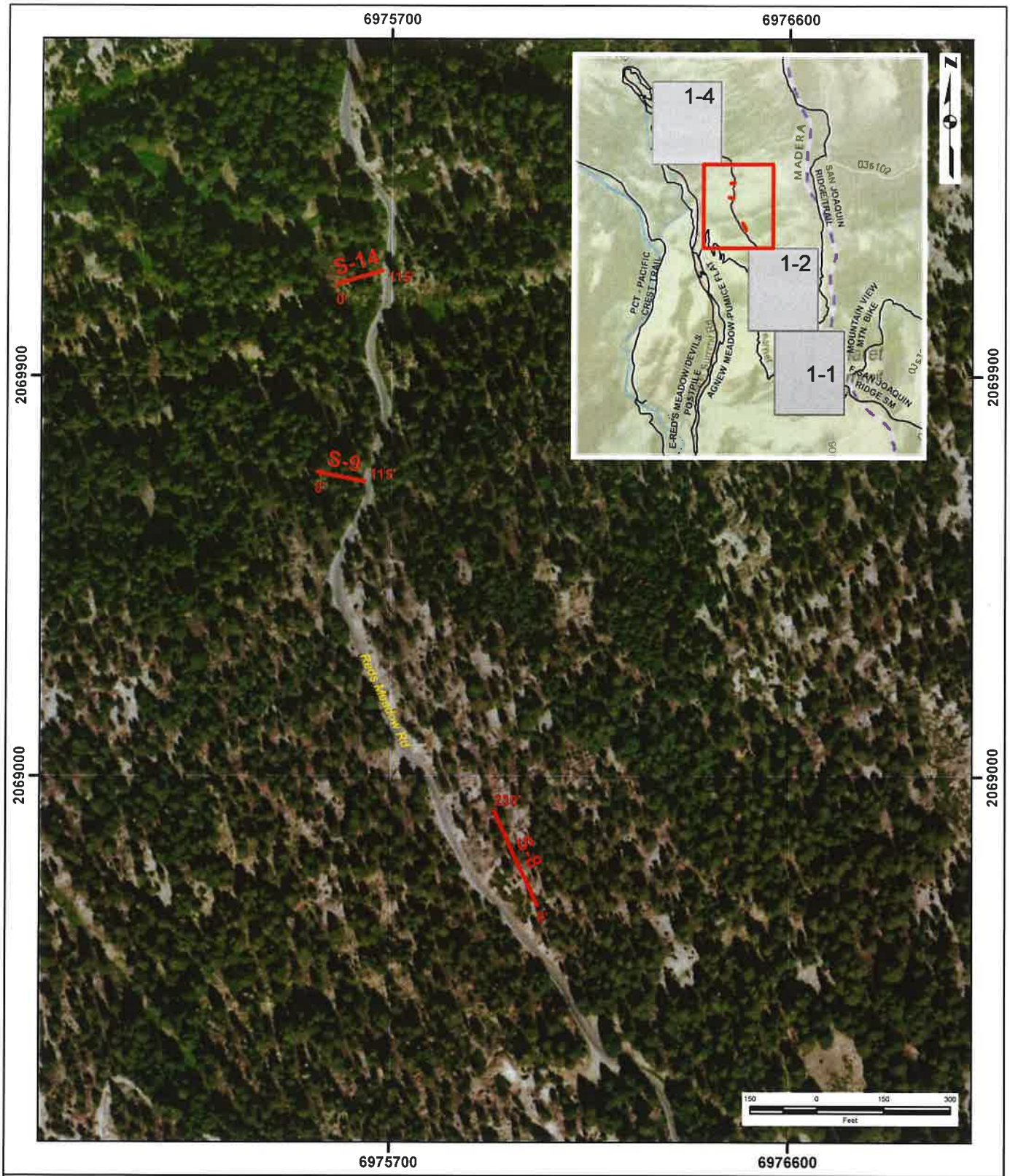

Legend

— P-wave Seismic Refraction Line

NOTES:
1. California State Plane Coordinate System, NAD 83, Zone III (0403), US Survey Feet
2. Base map source: Esri, DigitalGlobe, GeoEye, Earthstar Geographics, CNES/Airbus DS, USDA, USGS, AeroGRID, IGN, HERE, Garmin, Intermap, increment P Corp., GEBCO, FAO, NPS, NRCAN, GeoBase,Kadaster NL, Ordnance Survey, Esri Japan, METI, Esri China (Hong Kong), swisstopo, © OpenStreetMap contributors, and the GIS User Community

GEOVision geophysical services

Date:	11/7/2018
GV Project:	18419
Developed by:	D Carpenter
Drawn by:	T Rodriguez
Approved by:	W Dalrymple
File Name:	18419_1.MXD

FIGURE 1-3
S-8, S-9, S-14

SITE LOCATED NEAR
REDS MEADOW
MADERA COUNTY, CALIFORNIA

PREPARED FOR
SHANNON & WILSON, INC.

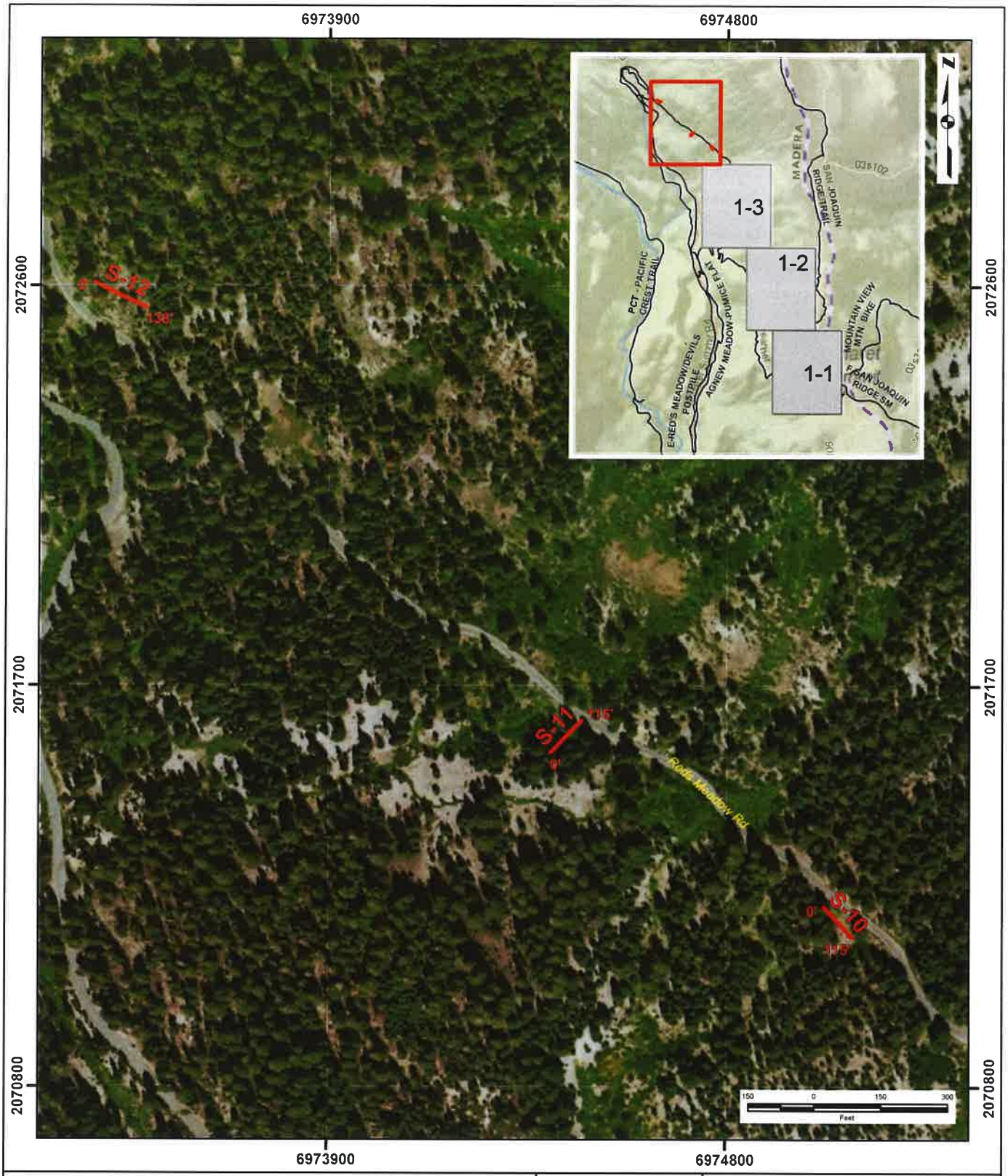

Legend

— P-wave Seismic Refraction Line

NOTES:
1. California State Plane Coordinate System, NAD 83, Zone III (0403), US Survey Feet
2. Base map source: Esri, DigitalGlobe, GeoEye, Earthstar Geographics, CNES/Airbus DS, USDA, USGS, AeroGRID, IGN, HERE, Garmin, Intermap, increment P Corp., GEBCO, FAO, NPS, NRCAN, GeoBase,Kadaster NL, Ordnance Survey, Esri Japan, METI, Esri China (Hong Kong), swisstopo, © OpenStreetMap contributors, and the GIS User Community

GEOVision geophysical services

Date:	11/7/2018
GV Project:	18419
Developed by:	D Carpenter
Drawn by:	T Rodriguez
Approved by:	W Dalrymple
File Name:	18419_1.MXD

FIGURE 1-4
S-10, S-11, S-12

SITE LOCATED NEAR
REDS MEADOW
MADERA COUNTY, CALIFORNIA

PREPARED FOR
SHANNON & WILSON, INC.

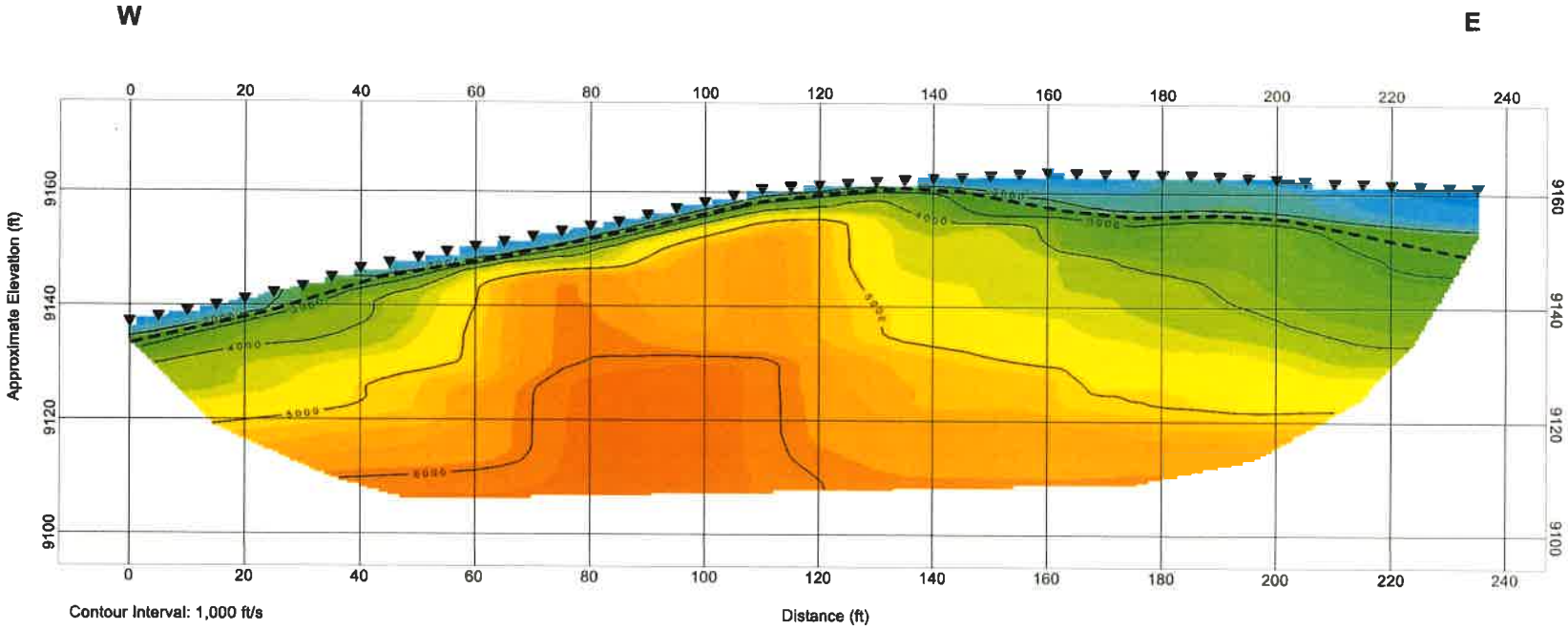

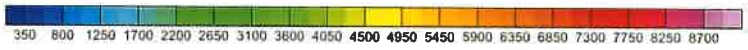

Legend

- ▼ Geophone Location
- - - Interpreted Contact between Fill/Colluvium and Bedrock

GEOVision geophysical services

Figure 2

S-1: P-wave Time-Term Tomography Model
GV Project No. 18419

Reds Meadow
Madera County, California

Prepared for Shannon & Wilson, Inc.

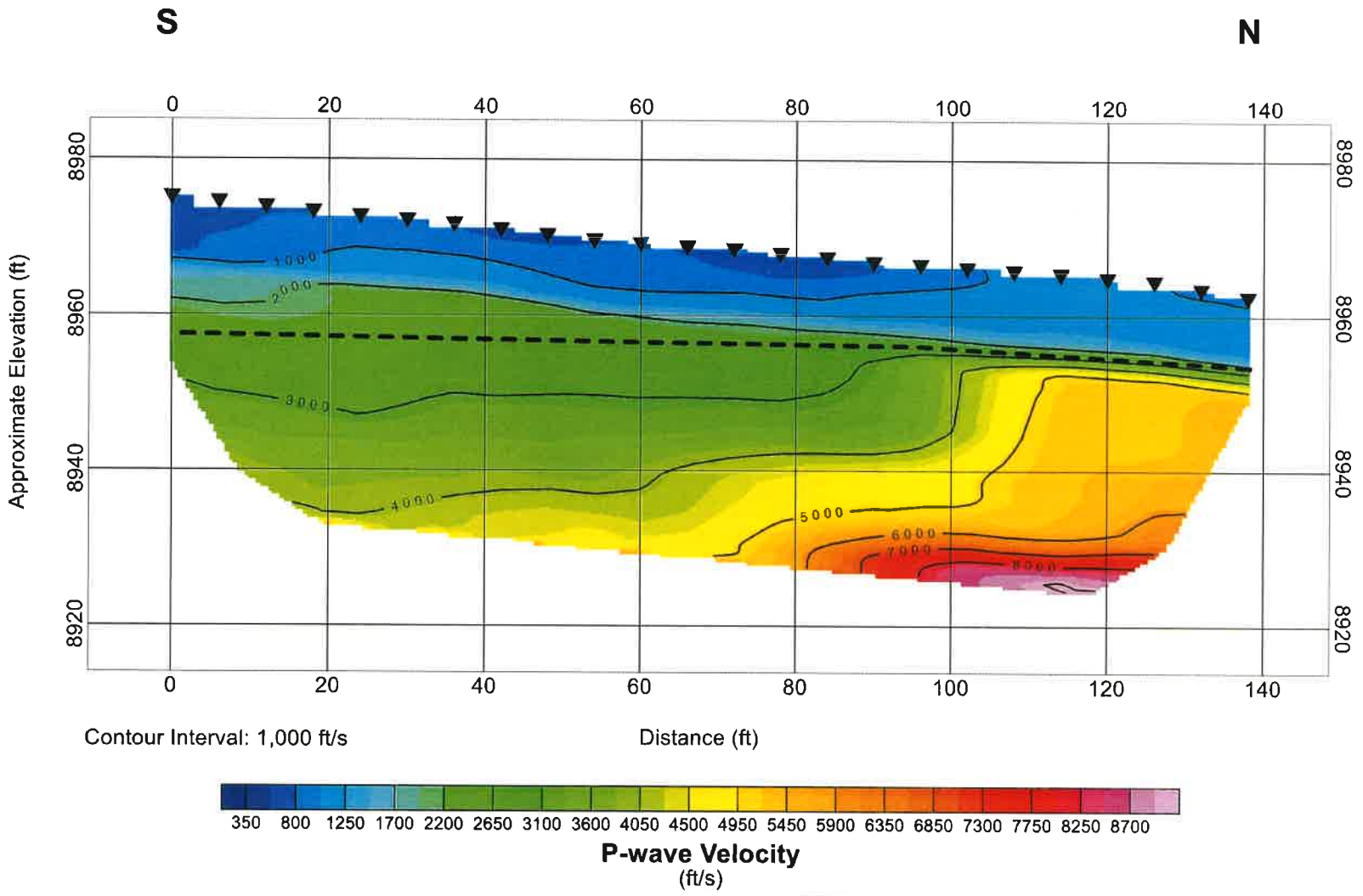

Legend

▼ Geophone Location

Interpreted Contact between Fill/Colluvium and Bedrock

10 0 10 20 30
(feet)

GEOVision geophysical services

Figure 3

S-2: P-wave Time-Term Tomography Model
GV Project No. 18419

Reds Meadow
Madera County, California

Prepared for Shannon & Wilson, Inc.

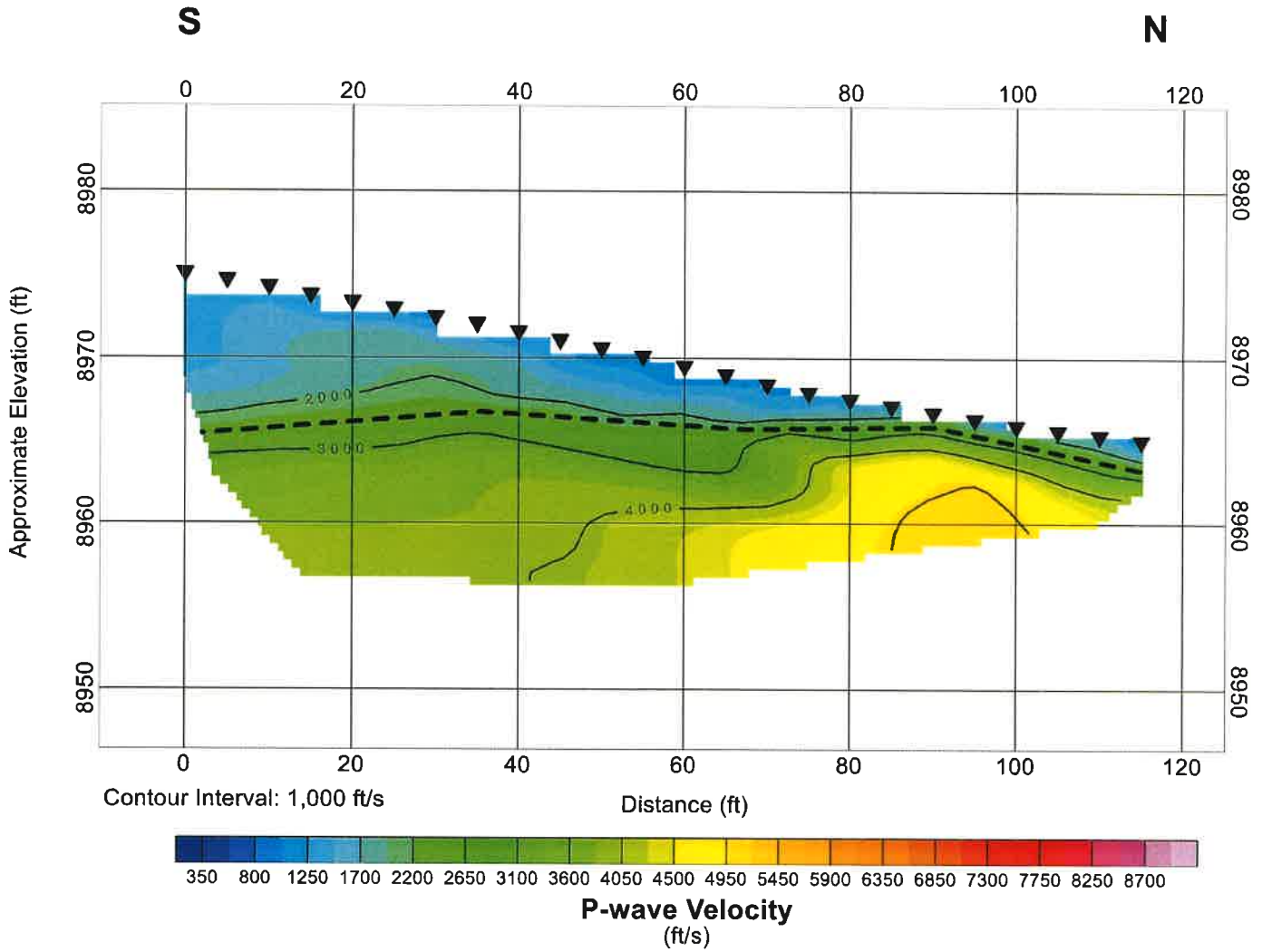

Legend

▼ Geophone Location

Interpreted Contact between Fill/Colluvium and Bedrock

10 0 10 20
(feet)

Vertical Exaggeration 2:1

GEOVision geophysical services

Figure 4

S-3: P-wave Time-Term Tomography Model
GV Project No. 18419

Reds Meadow
Madera County, California

Prepared for Shannon & Wilson, Inc.

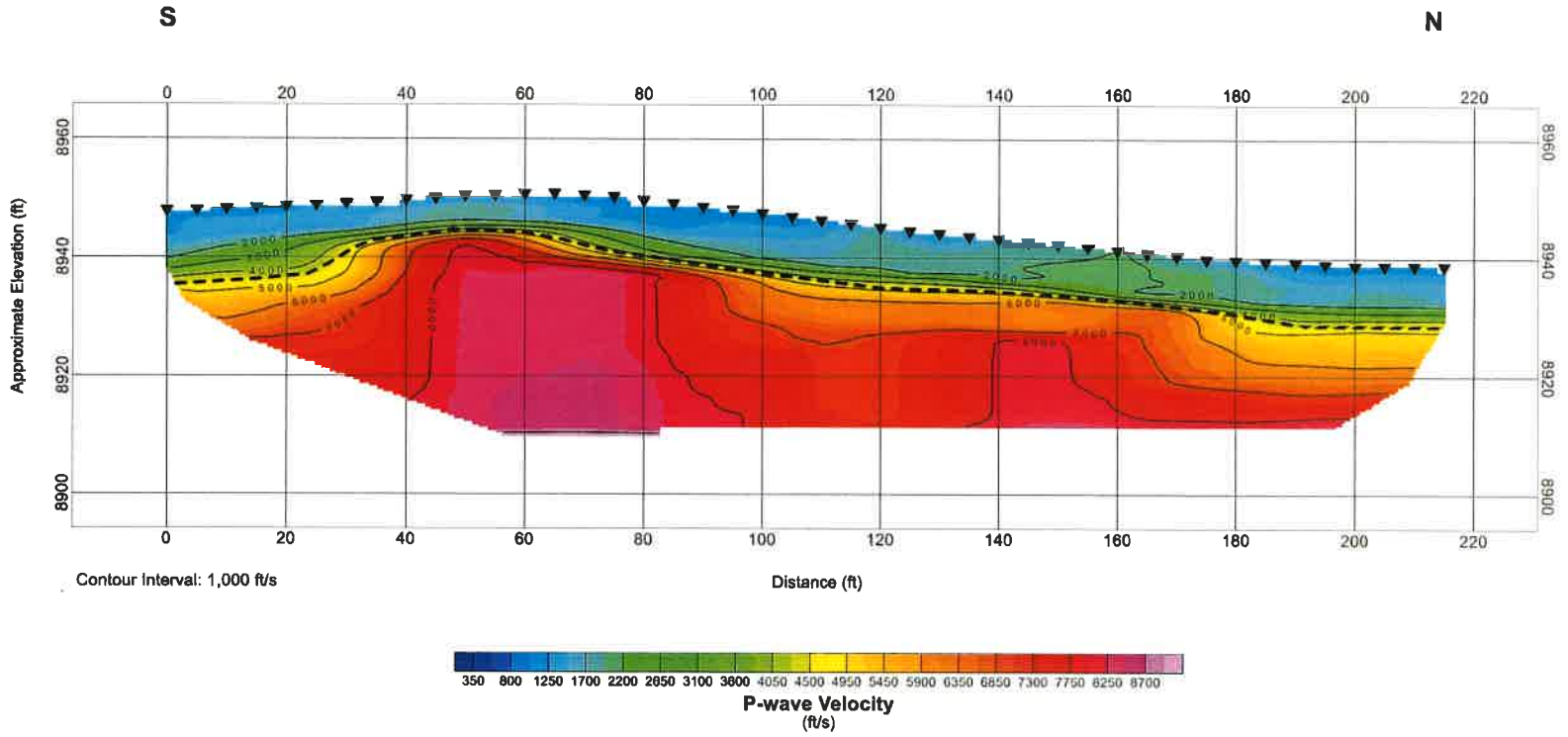

Legend

▼ Geophone Location

Interpreted Contact between Fill/Colluvium and Bedrock

10 0 10 20 30 40 50
(feet)

GEOVision geophysical services

Figure 5

S-4: P-wave Time-Term Tomography Model
GV Project No. 18419

Reds Meadow
Madera County, California

Prepared for Shannon & Wilson, Inc.

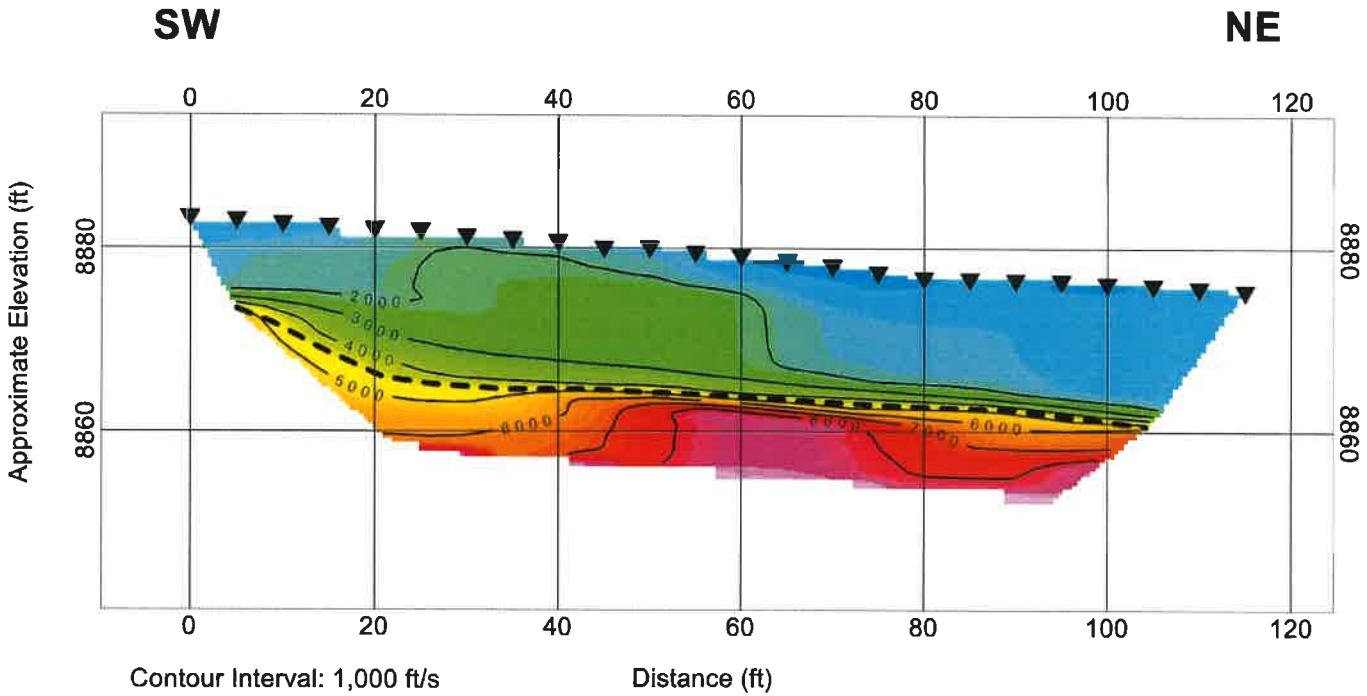

Legend

▼ Geophone Location

Interpreted Contact between Fill/Colluvium and Bedrock

10 0 10 20
(feet)

GEOVision geophysical services

Figure 6

S-5: P-wave Time-Term Tomography Model
GV Project No. 18419

Reds Meadow
Madera County, California

Prepared for Shannon & Wilson, Inc.

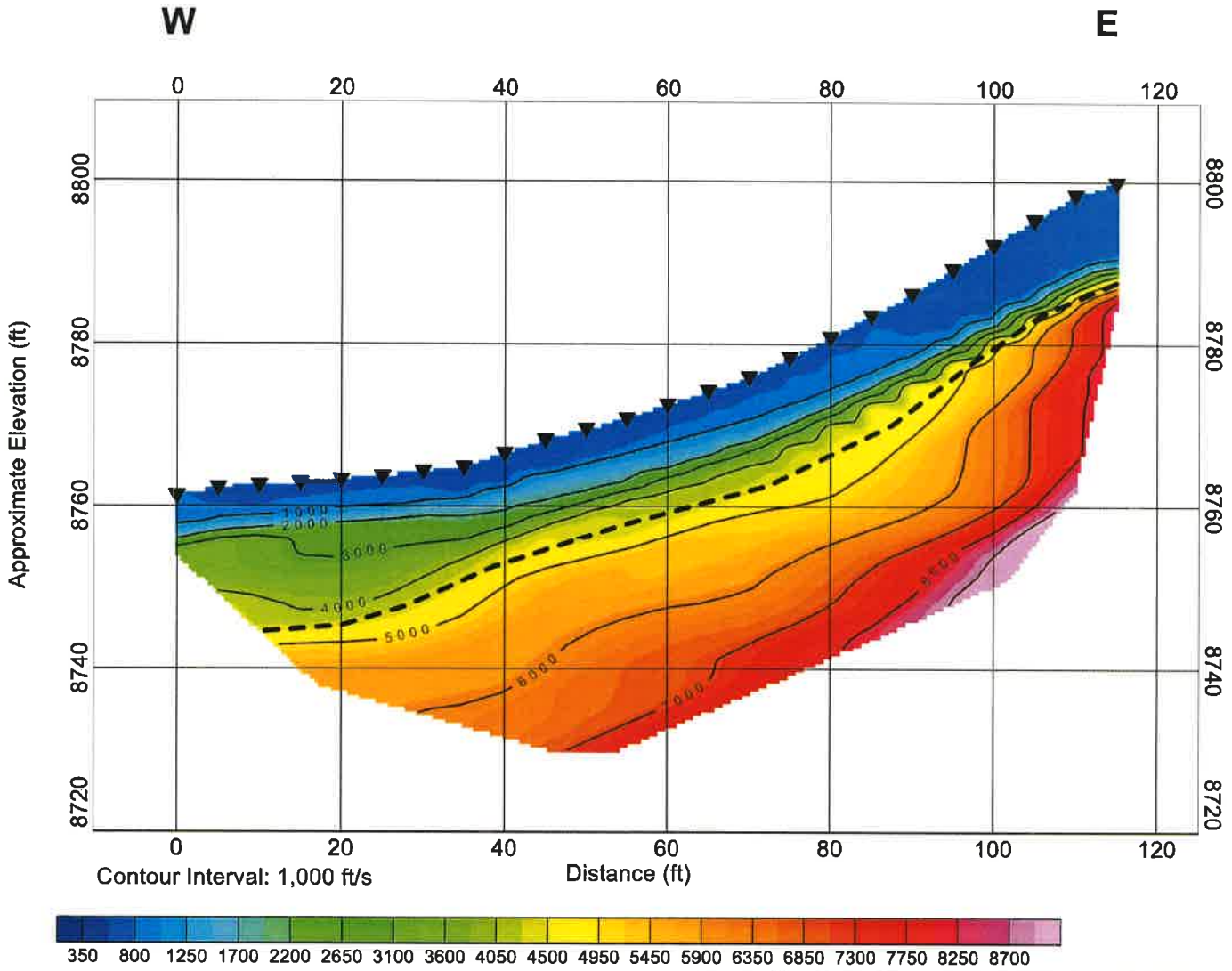

GEOVision geophysical services

Figure 7

S-6: P-wave Time-Term Tomography Model
GV Project No. 18419

Reds Meadow
Madera County, California

Prepared for Shannon & Wilson, Inc.

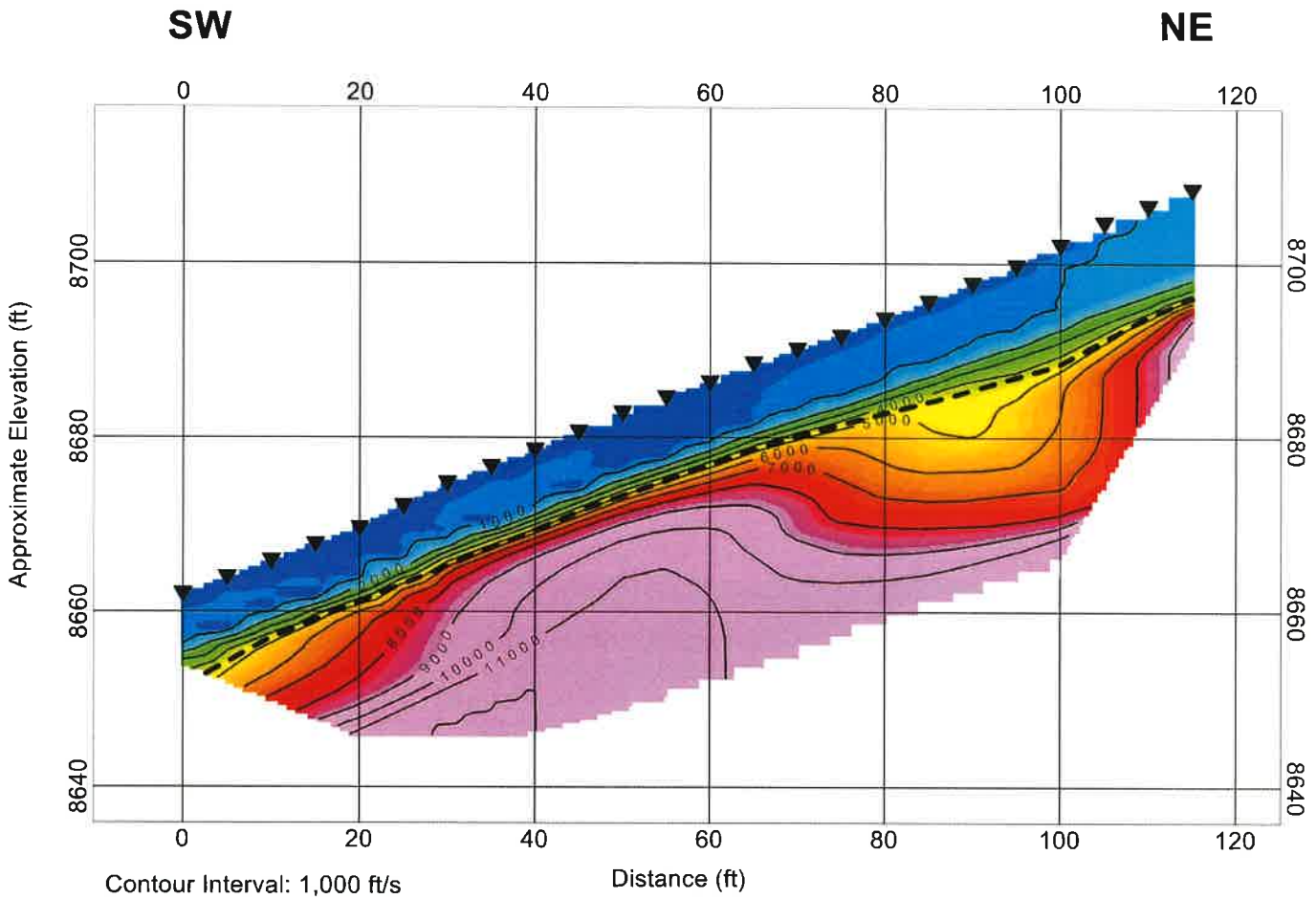

Legend

▼ Geophone Location

Interpreted Contact between Fill/Colluvium and Bedrock

10 0 10 20
(feet)

GEOVision geophysical services

Figure 8

S-7: P-wave Time-Term Tomography Model
GV Project No. 18419

Reds Meadow
Madera County, California

Prepared for Shannon & Wilson, Inc.

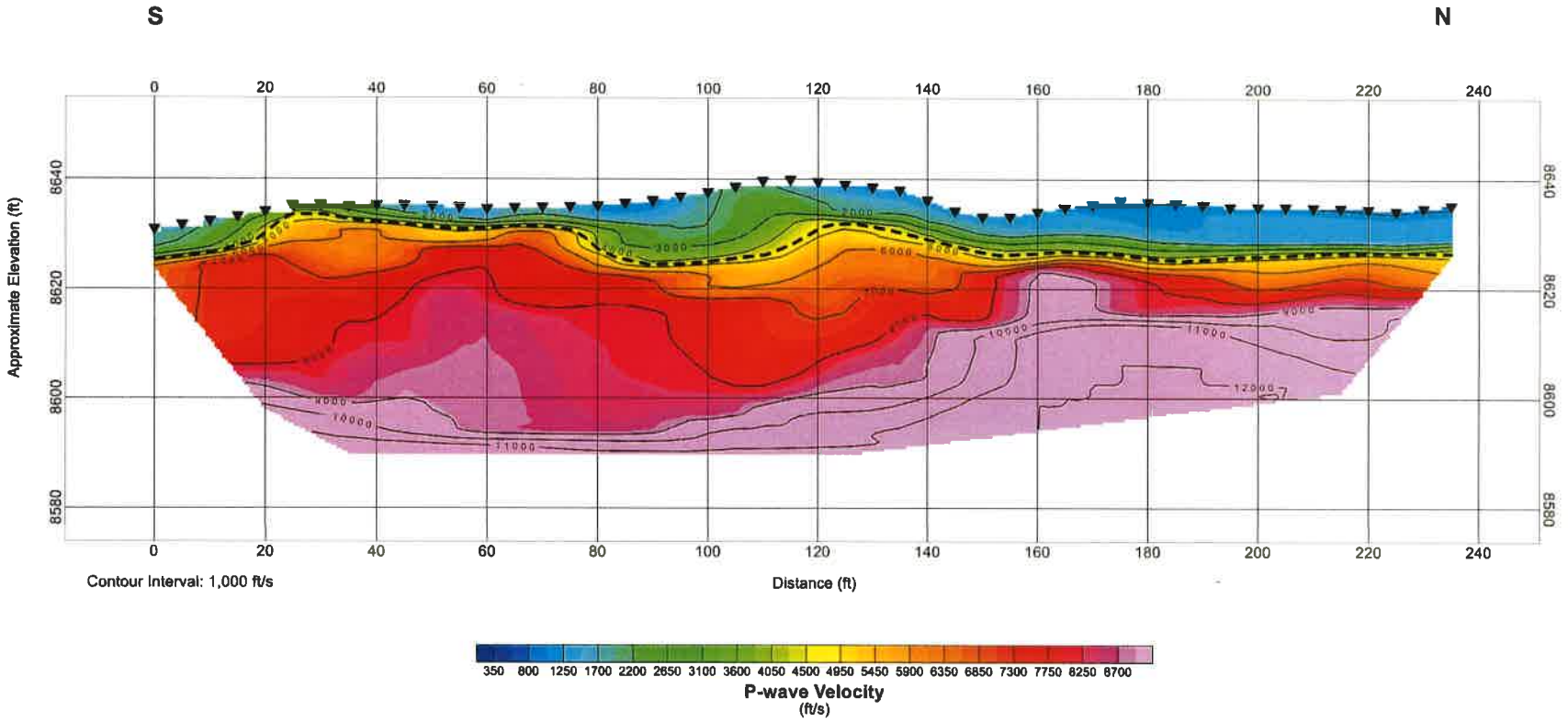

Legend

- ▼ Geophone Location
- Interpreted Contact between Fill/Colluvium and Bedrock

10 0 10 20 30 40 50
(feet)

GEOVision geophysical services

Figure 9

S-8: P-wave Time-Term Tomography Model
GV Project No. 18419

Reds Meadow
Madera County, California

Prepared for Shannon & Wilson, Inc.

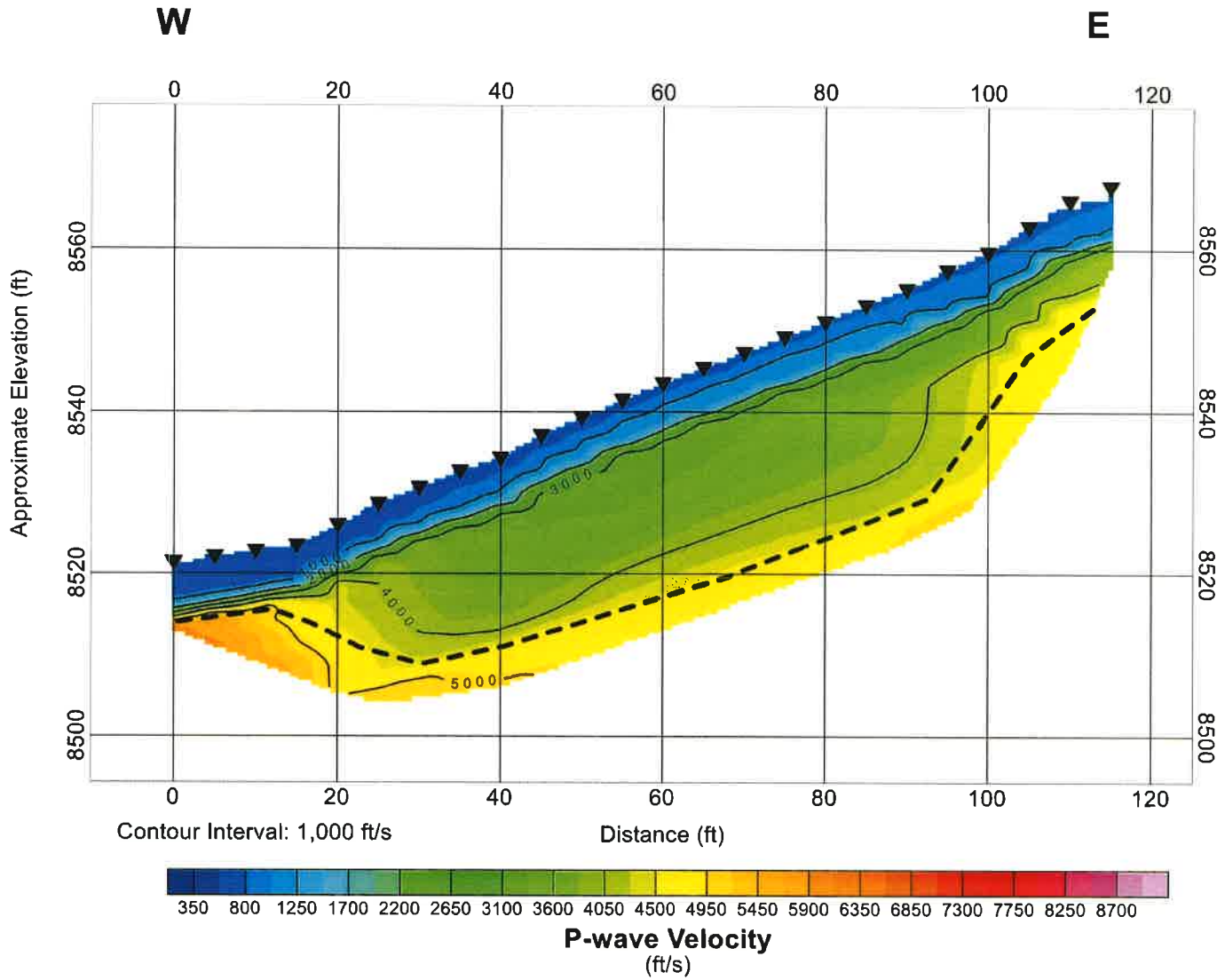

Legend

▼ Geophone Location

Interpreted Contact between Fill/Colluvium and Bedrock

10 0 10 20
(feet)

GEOVision geophysical services

Figure 10

S-9: P-wave Time-Term Tomography Model
GV Project No. 18419

Reds Meadow
Madera County, California

Prepared for Shannon & Wilson, Inc.

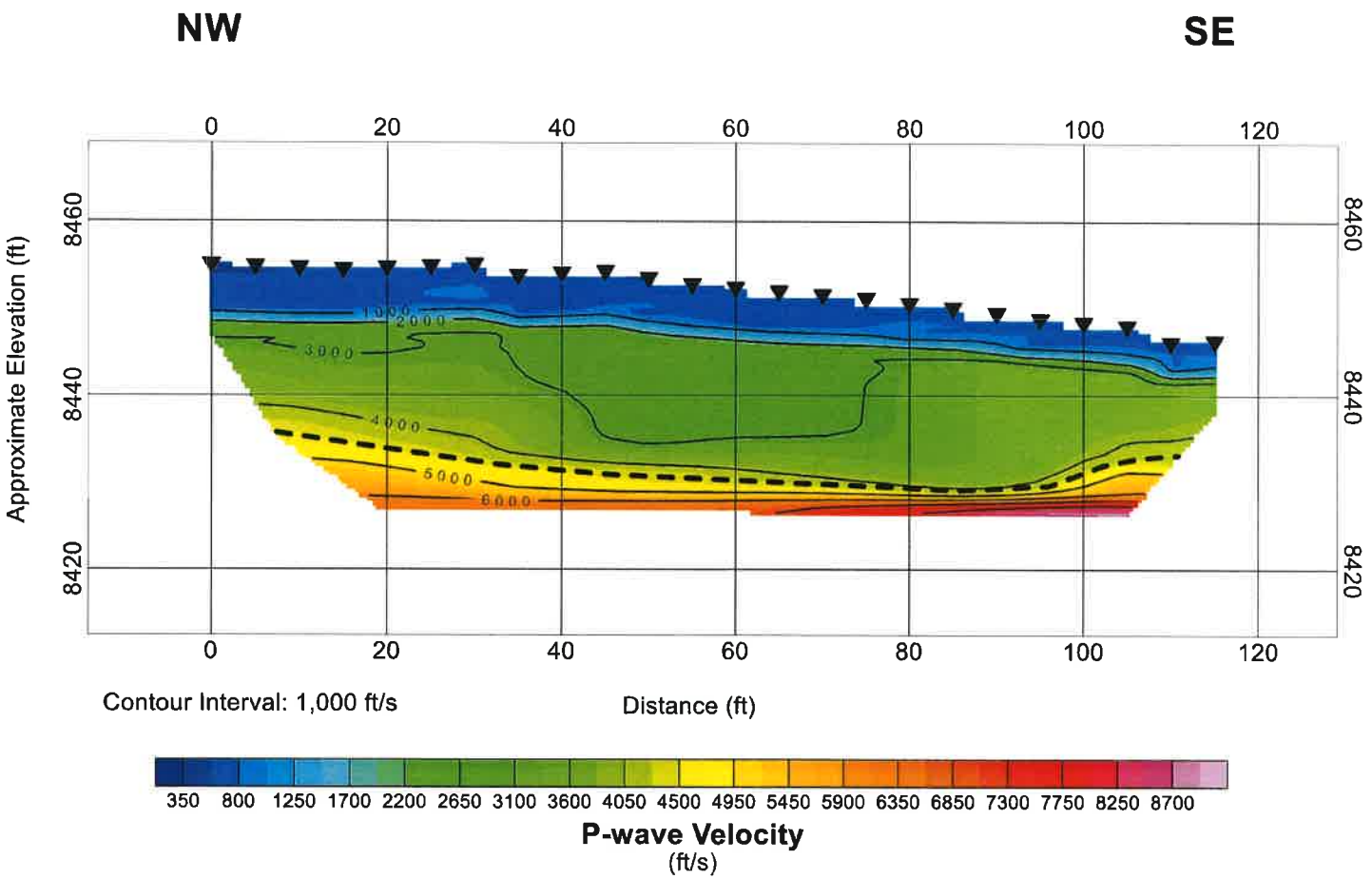

Legend

▼ Geophone Location

Interpreted Contact between Fill/Colluvium and Bedrock

10 0 10 20
(feet)

GEOVision geophysical services

Figure 11

S-10: P-wave Time-Term Tomography Model
GV Project No. 18419

Reds Meadow
Madera County, California

Prepared for Shannon & Wilson, Inc.

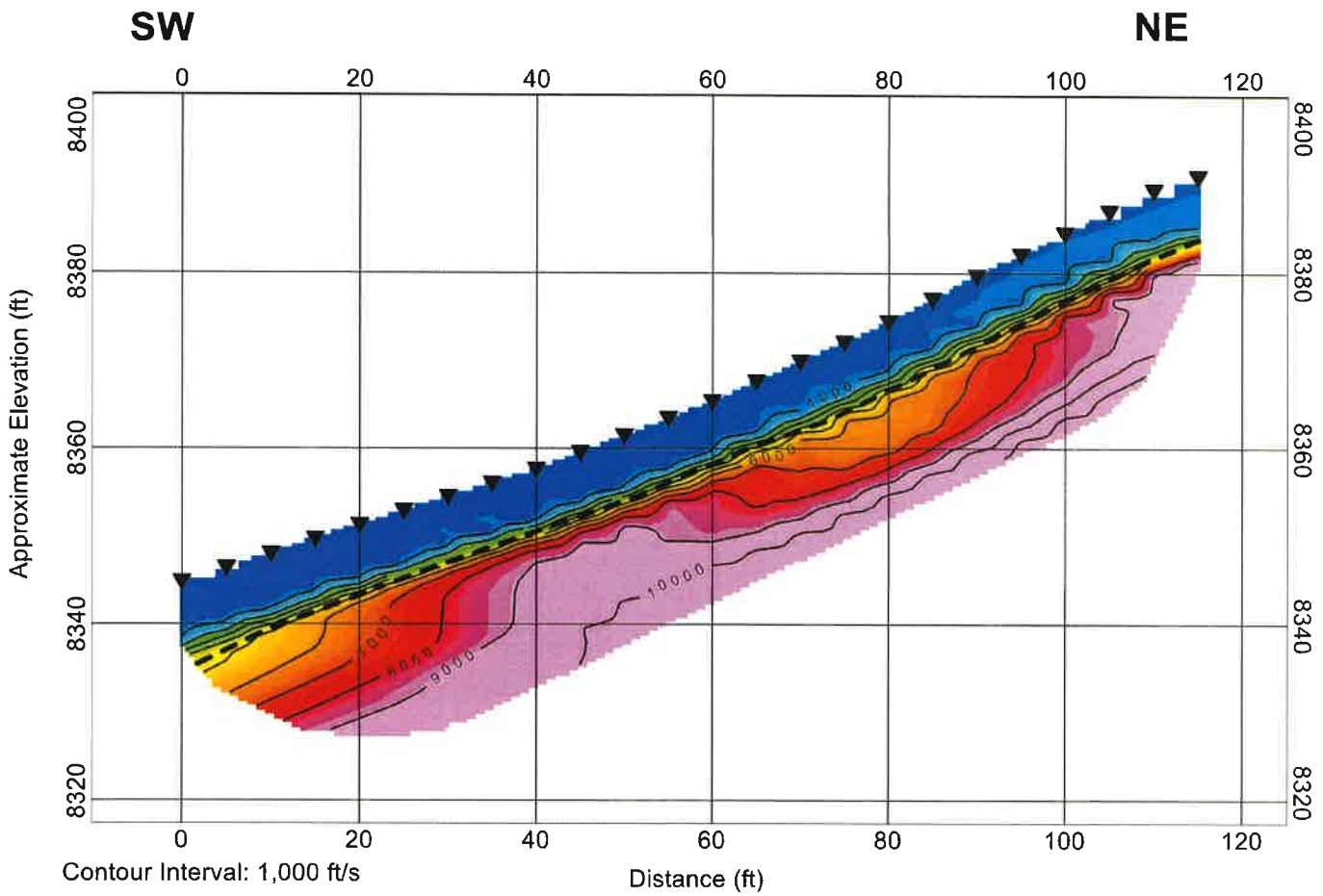

Legend

▼ Geophone Location

Interpreted Contact between Fill/Colluvium and Bedrock

10 0 10 20
(feet)

GEOVision geophysical services

Figure 12

S-11: P-wave Time-Term Tomography Model
GV Project No. 18419

Reds Meadow
Madera County, California

Prepared for Shannon & Wilson, Inc.

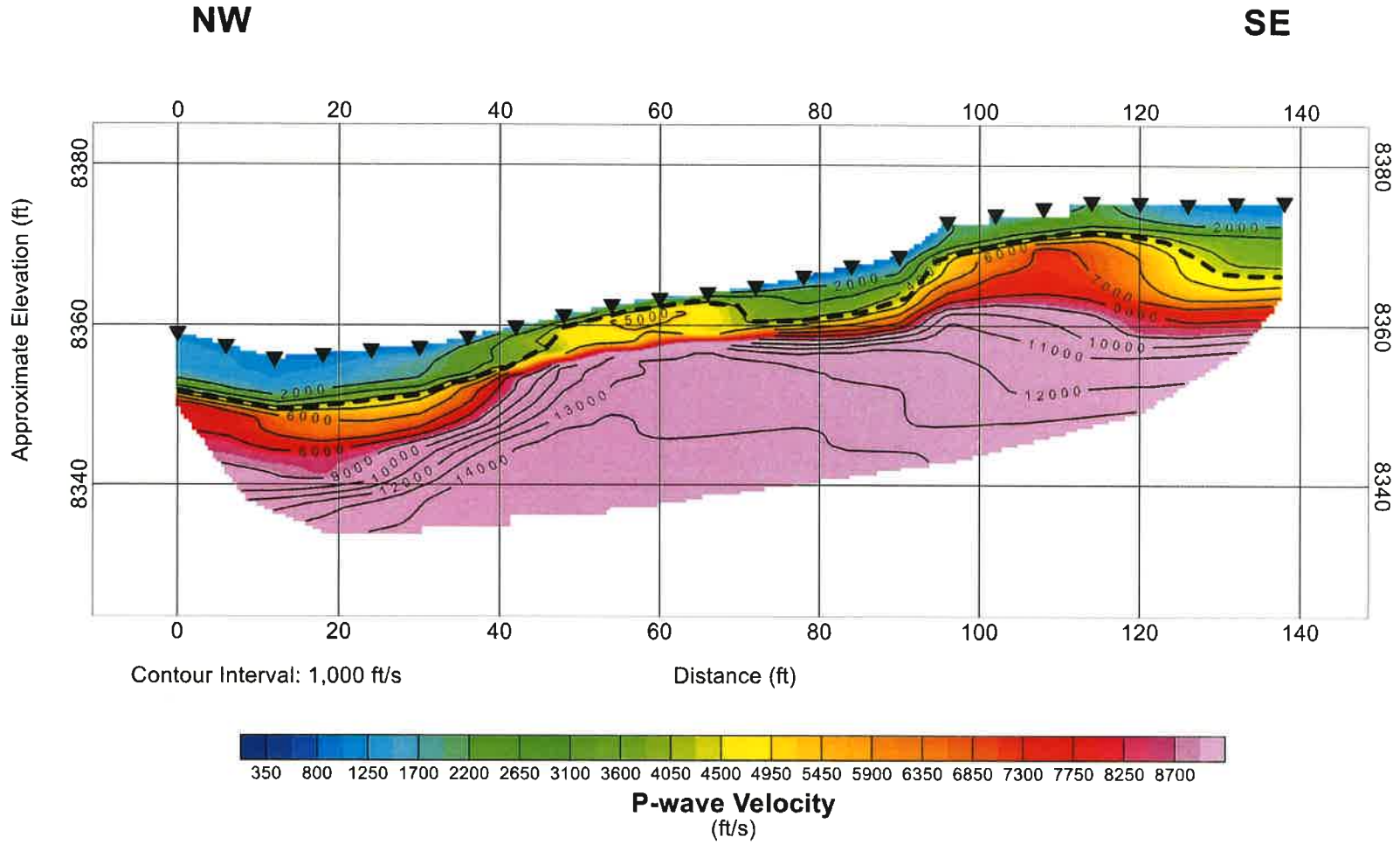

Legend

▼ Geophone Location

Interpreted Contact between Fill/Colluvium and Bedrock

10 0 10 20 30
(feet)

GEOVision geophysical services

Figure 13

S-12: P-wave Time-Term Tomography Model
GV Project No. 18419

Reds Meadow
Madera County, California

Prepared for Shannon & Wilson, Inc.

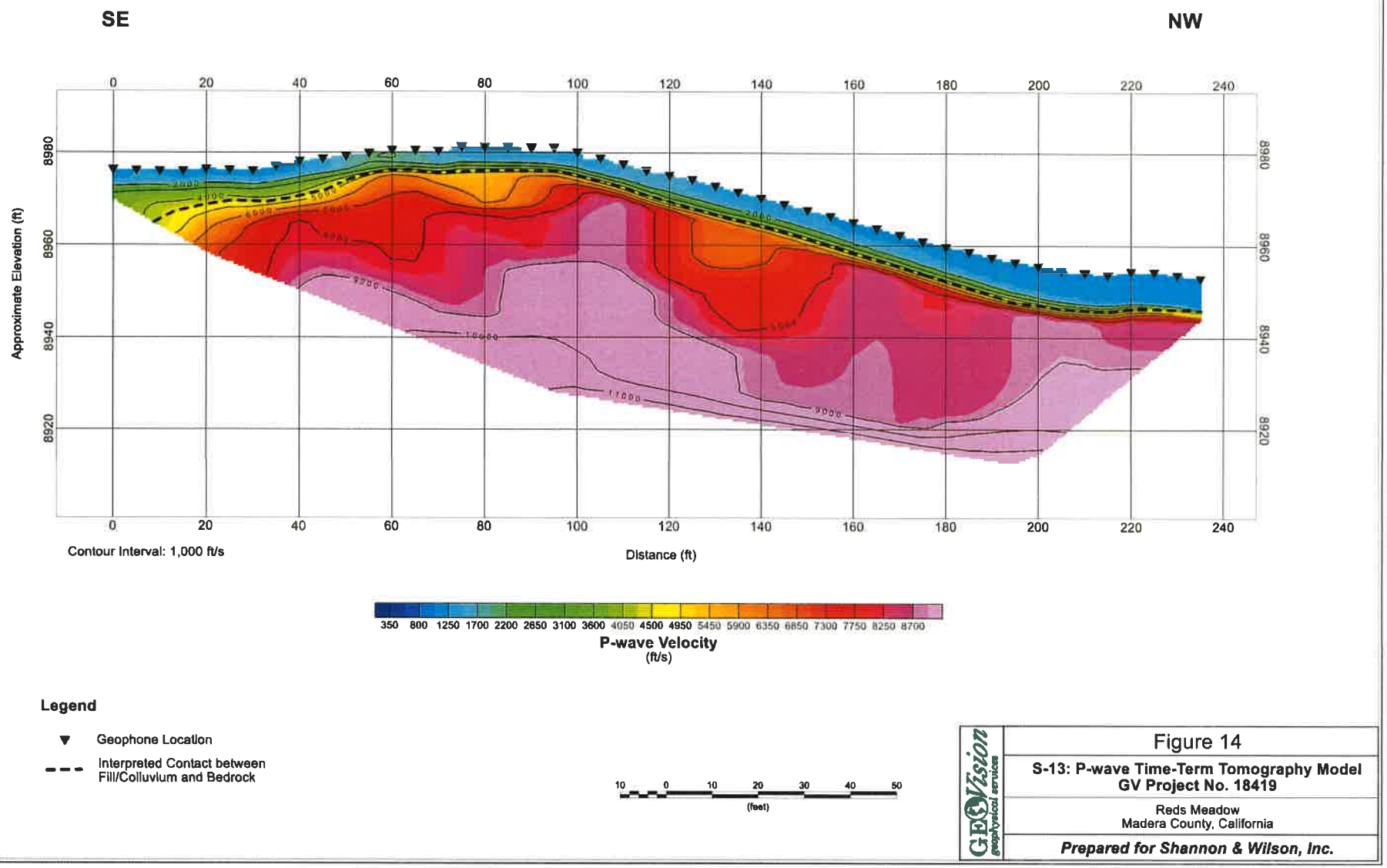

GEOVision geophysical services

Figure 14

S-13: P-wave Time-Term Tomography Model
GV Project No. 18419

Reds Meadow
Madera County, California

Prepared for Shannon & Wilson, Inc.

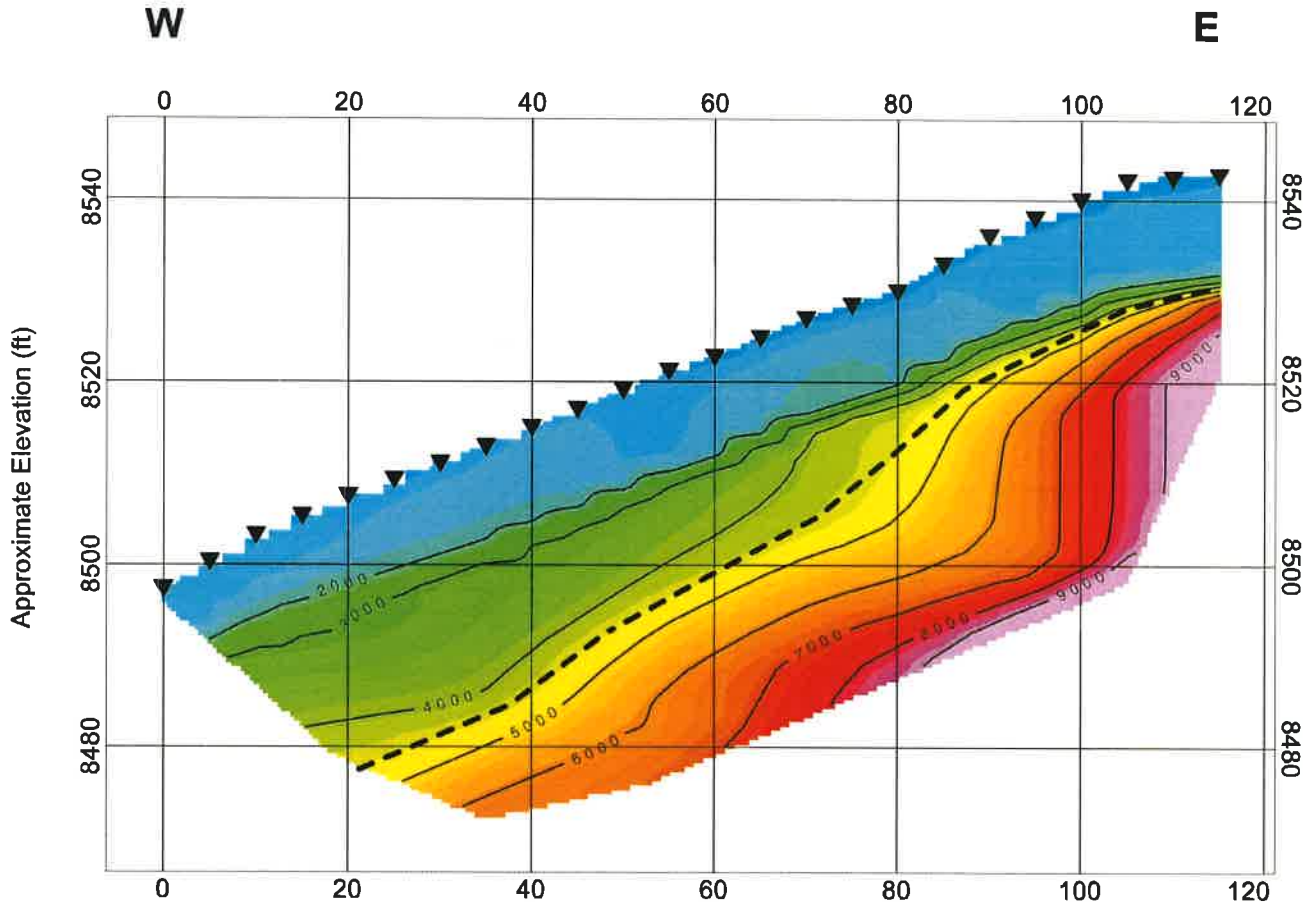

Legend

▼ Geophone Location

Interpreted Contact between Fill/Colluvium and Bedrock

10 0 10 20
(feet)

GEOVision geophysical services

Figure 15

S-14: P-wave Time-Term Tomography Model
GV Project No. 18419

Reds Meadow
Madera County, California

Prepared for Shannon & Wilson, Inc.

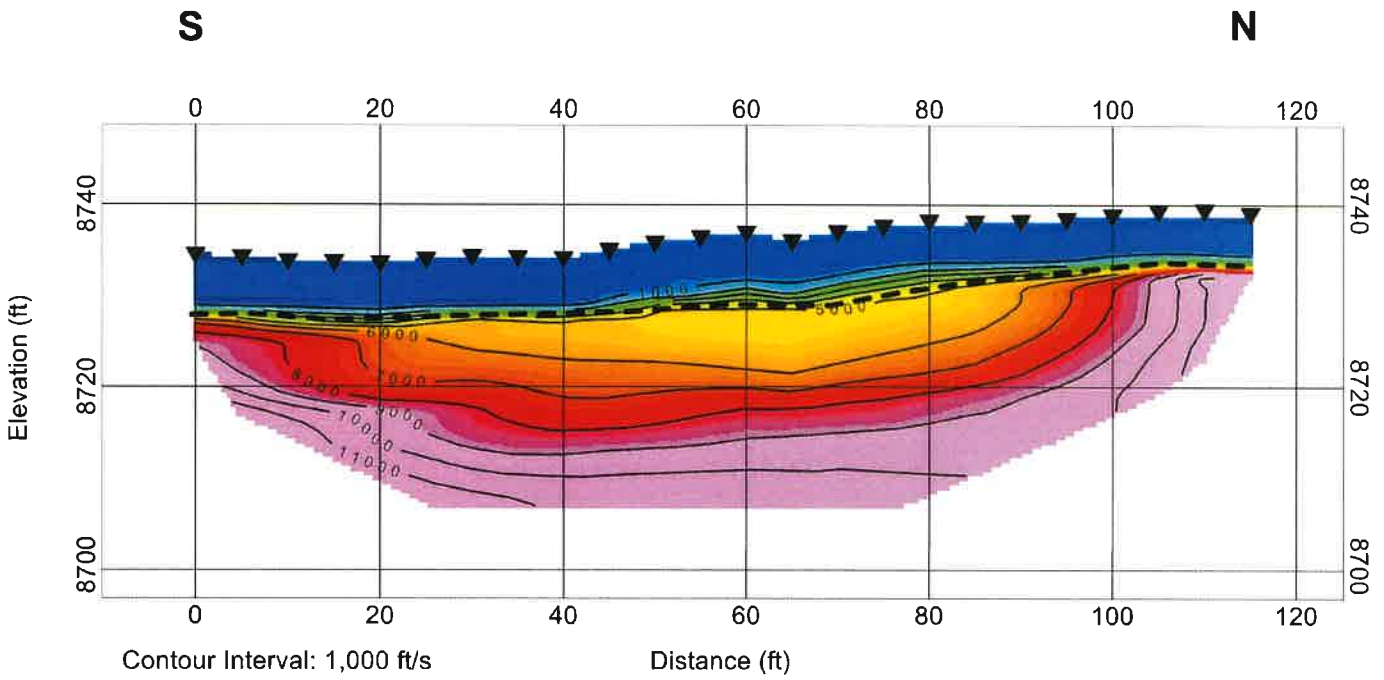

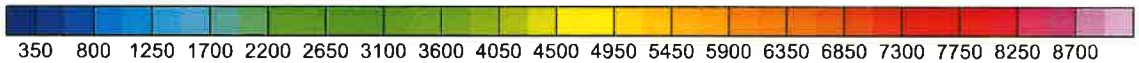

P-wave Velocity
(ft/s)

Legend

▼ Geophone Location

Interpretated Contact between Fill/Colluvium and Bedrock

10 0 10 20
(feet)

GEOVision geophysical services

Figure 16

S-15: P-wave Time-Term Tomography Model
GV Project No. 18419

Reds Meadow
Madera County, California

Prepared for Shannon & Wilson, Inc.

APPENDIX A

SEISMIC REFRACTION METHOD

GEO*Vision* geophysical services

GEO*Vision* conducts high-resolution seismic refraction and seismic reflection surveys in support of a variety of engineering, environmental, and hydrogeologic investigations.

When conducting seismic surveys, acoustic energy is input to the subsurface by an energy source such as a sledgehammer impacting a metallic plate, weight drop, vibratory source, or explosive charge. The acoustic waves propagate into the subsurface at a velocity dependent upon the elastic properties of the material through which they travel. When the waves reach an interface where the density or velocity changes significantly, a portion of the energy is reflected back to the surface, and the remainder is transmitted into the lower layer. Where the velocity of the lower layer is higher than that of the upper layer, a portion of the energy is also critically refracted along the interface. Critically refracted waves travel along the interface at the velocity of the lower layer and continually refract energy back to surface. Receivers (geophones), laid out in linear array on the surface, record the incoming refracted and reflected waves. The seismic refraction method involves analysis of the travel times of the first energy to arrive at the geophones. These first arrivals are from either the direct wave (at geophones close to the source), or critically refracted waves (at geophones further from the source). The seismic reflection method involves the analysis of reflected waves, which occur later in the seismic record.

GEO*Vision* uses the seismic refraction method to:

- **Map bedrock topography**
- **Map depth to groundwater**
- **Map faults in bedrock**
- **Map faults forming groundwater barriers**
- **Characterize landslides**
- **Estimate bedrock rippability**
- **Evaluate soil and rock properties**

Seismic Refraction Survey in Mojave Desert, California using XLR8 2700 lb Accelerated Weight Drop Energy Source

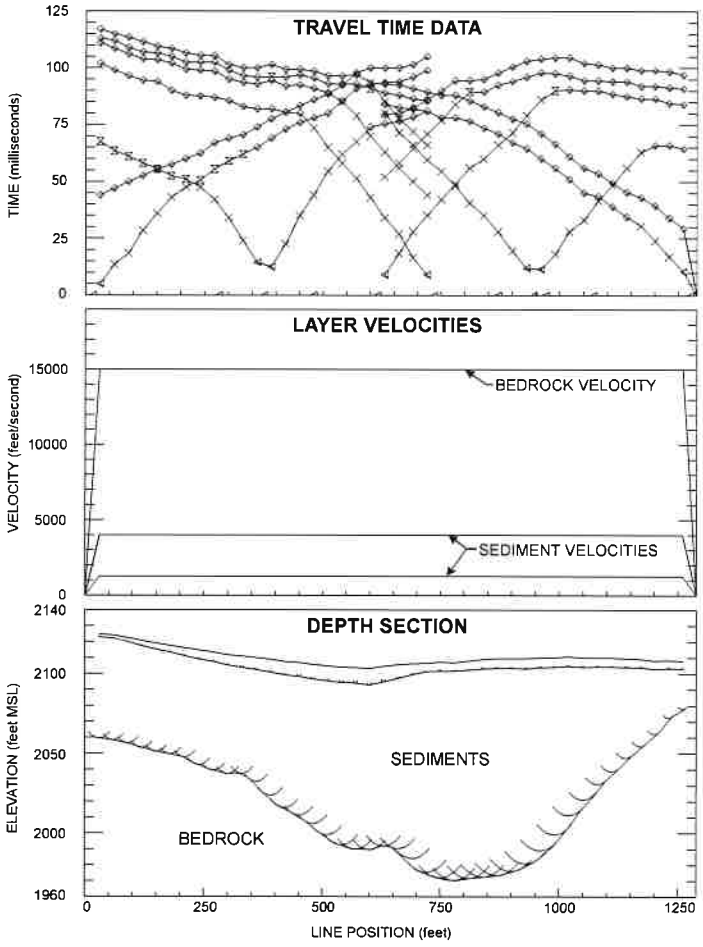

Seismic Refraction Survey to Map Bedrock Topography

1124 Olympic Drive, Corona, California 92881 ph 951-549-1234 fx 951-549-1236 www.geovision.com

GEO*Vision* seismic refraction equipment includes:

- Multiple Geometrics Geode 24-channel seismographs
- Oyo DAS-1 seismograph with 144-channel capability
- Seismic refraction cables with 10 to 55 ft takeouts
- 4.5, 8 and 10 Hz geophones
- 40 and 100 kg accelerated weight drop energy sources
- Betsy downhole percussion firing rod
- Seismic Source and Gisco radio trigger modules
- High-voltage blaster

100 kg Accelerated Weight Drop

Geometrics Geode Seismographs

Analysis of seismic refraction data depends upon the complexity of the subsurface seismic velocity structure. If the subsurface target is planar in nature then the slope intercept method can be used to model multiple horizontal or dipping planar layers. A minimum of one end shot is required to model horizontal layers and reverse end shots are required to model dipping planar layers. If the subsurface target is undulating and exhibits an abrupt velocity increase (e.g. basement surface) then layer based analysis routines such as the generalized reciprocal method, delay time method, time-term method, plus-minus method and wavefront method are required to model subsurface velocity structure. These methods generally require a minimum of 5 to 7 shot points per spread (end shots, off end shots and a center shot). If subsurface velocity structure is complex and cannot be adequately modeled using layer-based modeling techniques (e.g., complex weathering profile in bedrock, numerous lateral velocity variations), then tomographic inversion techniques are best suited to model the seismic refraction data. These techniques require a high shot density (typically every 2 to 6 stations/ geophones).

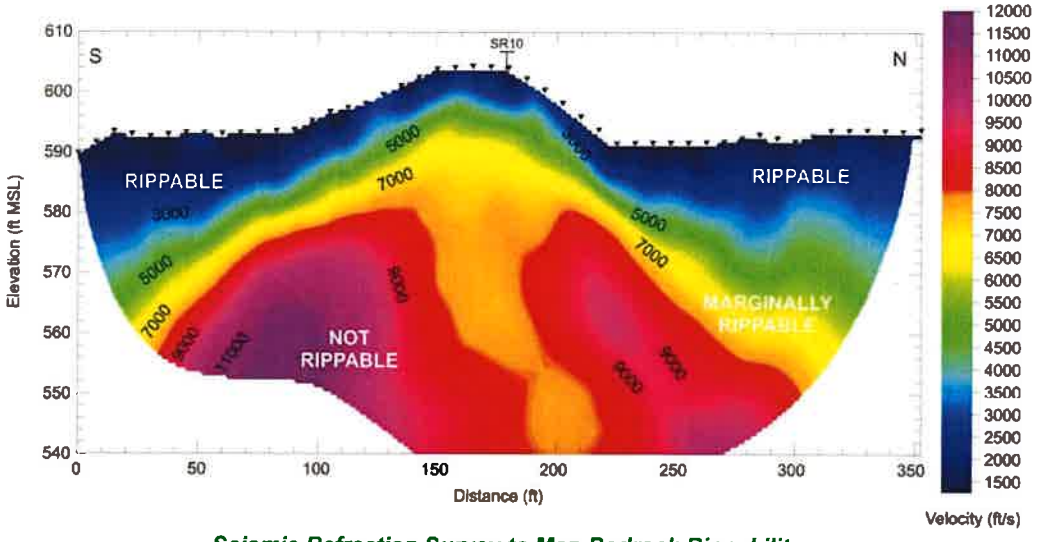

Seismic Refraction Survey to Map Bedrock Rippability

GEO*Vision* maintains several software packages to model seismic refraction data including:

- Firstpix™ by Interpex, Ltd.
- IXrefraX by Interpex ,Ltd.
- Viewseis™ by Viewlog Systems, Ltd.
- Refract by Geogiga
- Seisimager™ by Geometrics, Inc./Oyo Corporation
- Rayfract™ by Intelligent Resources, Inc.
- SeisOpt™ Pro by Optim LLC

These software packages allow processing of seismic refraction data using the following layer based and smooth velocity model techniques:

- Generalized reciprocal method (GRM)
- Reciprocal method/delay time method
- Time-Term method
- Plus-Minus method
- Wavefront method
- Monte Carlo based inversion
- Delta t-V tomographic inversion
- Wavepath Eikonal traveltime tomographic inversion
- Nonlinear traveltime tomographic analysis

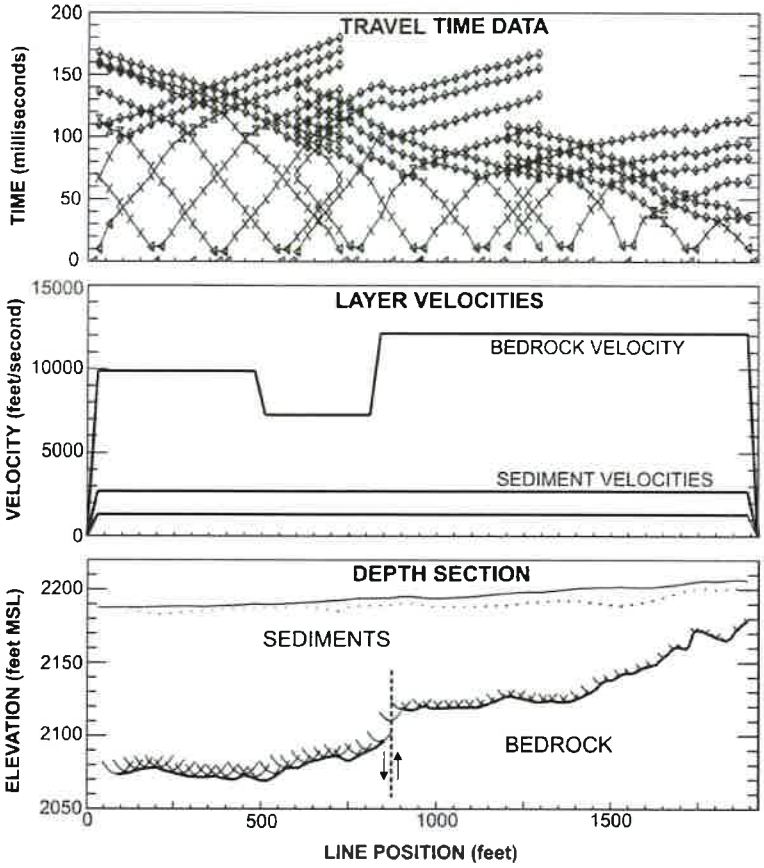

Seismic Refraction Survey to Map Bedrock Fault

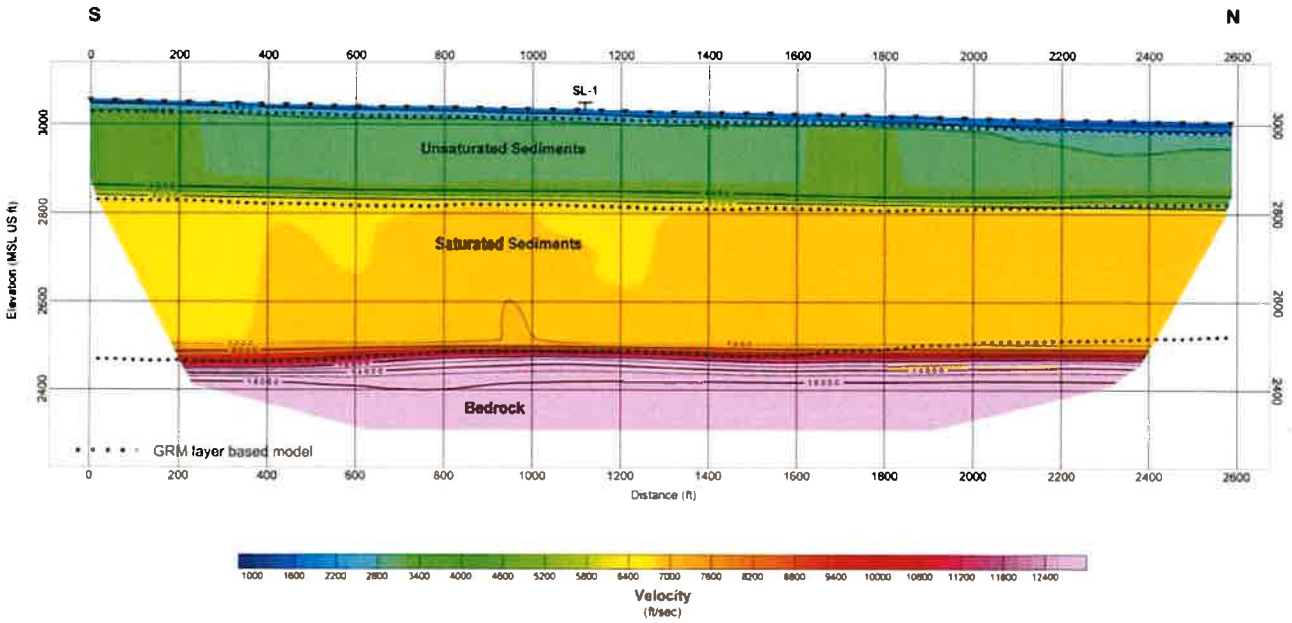

Seismic Refraction Survey to Map Depth to Groundwater (200 ft deep) and Bedrock (500 to 600 ft deep) as part of a Groundwater Resources Investigation. Energy Source Consisted of XLR8 2700 lb Accelerated Weight Drop. Data modeled using Nonlinear Traveltime Tomographic Analysis with a Layer-Based Starting Model.

1124 Olympic Drive, Corona, California 92881 ph 951-549-1234 fx 951-549-1236 www.geovision.com

Drilling Shot Holes for Explosive Seismic Refraction Survey

Loading Explosive Charge

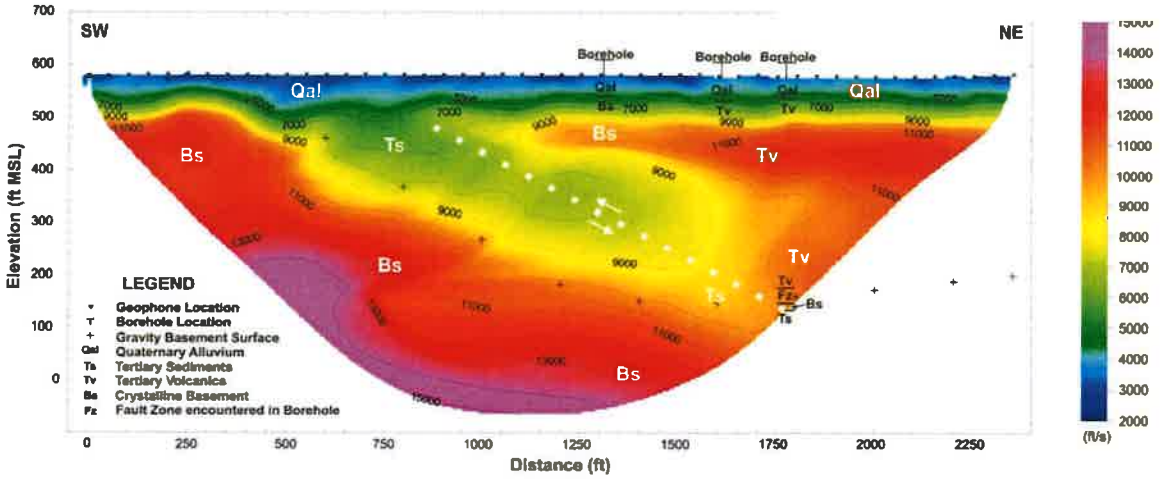

Seismic Refraction Imaging of Complex Geologic Structure consisting of Tertiary Volcanic Rocks and Basement Rocks Thrust over Tertiary Sediments and Basement Complex. Small Explosive Charges used as the Energy Source and Data Modeled using Wavepath Eikonal Traveltime Tomographic Inversion.

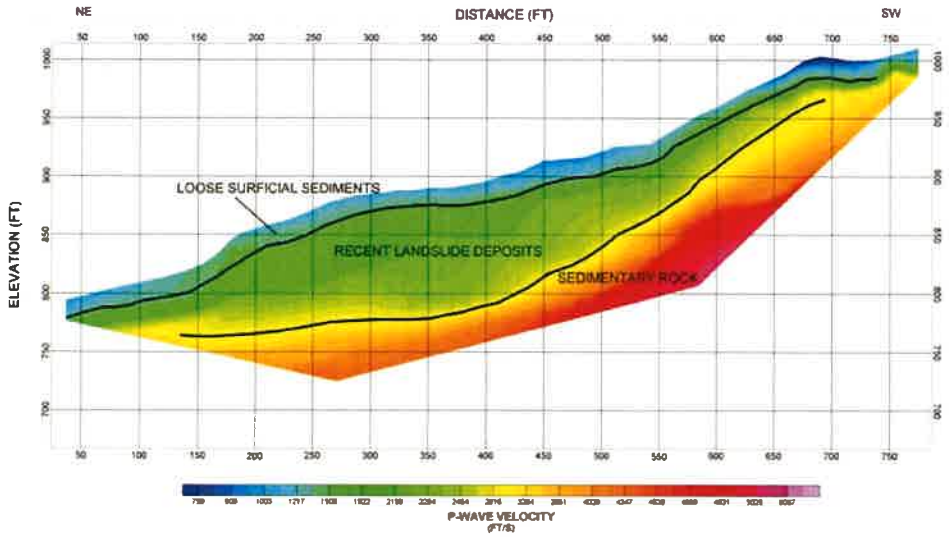

Seismic Refraction Survey to Characterize a Landslide

1124 Olympic Drive, Corona, California 92881 ph 951-549-1234 fx 951-549-1236 www.geovision.com